Université du Québec
à Rimouski

EFFETS DES APPORTS FLUVIAUX EN NUTRIMENTS AZOTÉS SUR LA COMPOSITION ETLES FLUX VERTICAUX DES PARTICULES MICROBIENNES DANS L'ESTUAIRE MARITIME DU SAINT-LAURENT

Mémoire présenté

dans le cadre du programme de maîtrise en océanographie

en vue de l'obtention du grade de maître ès sciences (M.Sc.)

PAR

© JADE PARADIS-HAUTCOEUR

avril 2021

Composition du jury :

Christian Nozais, président du jury, Université du Québec à Rimouski

Michel Gosselin, directeur de recherche, Institut des sciences de la mer de Rimouski

Michel Starr, codirecteur de recherche, Institut Maurice-Lamontagne

Éric Fouilland, examinateur externe, Unité Mixte de Recherche MARBEC

Dépôt initial le 21 décembre 2020 Dépôt final le 19 avril 2021

REMERCIEMENTS

Un immense merci à mon directeur de recherche Michel Gosselin et mon co-directeur Michel Starr. Je vous remercie de votre implication et de votre enthousiasme envers le projet du début jusqu'à la fin. Nos rencontres hebdomadaires depuis le début de la pandémie ont su me garder motivée. Votre curiosité scientifique et votre passion pour la recherche est inspirante. Mon parcours à la maîtrise a été grandement formateur grâce à vous, j'ai eu l'opportunité de faire plusieurs missions d'échantillonnage en mer et d'apprendre plusieurs méthodes d'analyse en laboratoire.

Merci à toute l'équipe de SECO.Net : À Gabrièle Deslongchamps pour la coordination du projet ; Vincent Villeneuve pour les données de nutriments ; Liliane St-Amand pour la préparation de matériel et l'aide en laboratoire ; Karine Lemarchand pour l'aide et les conseils ; David Lévesque, Sylvie Saint-Pierre et Michel Lebeuf pour les données de matière organique ; Michael Scarratt, Sonia Michaud et Jean-Yves Couture pour avoir fourni une liste des espèces présentes dans les échantillons.

Merci aux équipes techniques des divers instituts de recherche : Mélanie Simard, Pascal Rioux, Bruno Cayouette, Christian Boutot, Nathalie Morin, Jonathan Gagnon, Jonathan Coudé, Kim Doiron, Mathieu Milour et plusieurs autres pour leur aide précieuse tant sur le terrain qu'en laboratoire.

Merci aux étudiantes Océane Reignier, Amélie Évrard, Delphine Béland, Jenny Lapierre, Joannie Charette, Virginie Galindo, Aude Boivin-Rioux, Coralie Voyer d'avoir autant travaillé pour m'aider le jour, le soir comme la fin de semaine soit pour m'expliquer des protocoles, laver (et relaver !) des mésocosmes, préparer du matériel ou analyser des échantillons. Un merci particulier à Constance Duffaud, coéquipière de terrain hors pair.

Merci à Alain Caron, Fanny Noisette et David Deslauriers, ce n'est pas facile les statistiques, une chance que vous êtes là !

Merci Catherine Lalande d'avoir lu et relu ce mémoire pour m'aider à mieux écrire et merci à Christian Nozais et Éric Fouilland de corriger ce mémoire en tant que président et membre externe du jury.

Merci à l'Institut des sciences de la mer de Rimouski et à son équipe administrative incroyable : Martine Belzile, Nancy Lavergne, Brigitte Dubé et Marielle Lepage.

Merci à Jean-Christophe Hautcoeur pour le graphisme des affiches et schémas.

Merci à l'estuaire du Saint-Laurent d'être aussi fascinant et à Anna de me permettre de le naviguer.

Sur une note plus personnel, si mon parcours à la maîtrise sera inoubliable c'est surtout grâce aux amitiés. Merci à tout-e-s les némoïdes qui rendent la vie étudiante si intéressante. Alana, Catherine, Marie-Pier et Valérie merci d'être là, vous êtes des scientifiques et des femmes incroyables. Merci Éléonore, Ida, Maude, Tais et Rosalie, vivement la fin de la pandémie pour toutes vous revoir ! Merci à ma grand-mère, mes parents et ma sœur pour le soutien et l'encouragement. Et surtout, merci à Alexis, merci d'avoir déménager à Rimouski pour ce projet et merci de m'avoir rappelé l'importance de prendre des pauses.

Finalement merci aux programmes subventionnaires qui ont cru en la pertinence du projet en le finançant : Programme de contribution à la recherche scientifique sur les océans et les eaux douces du ministère des Pêches et des Océans du Canada, le Conseil de recherches en sciences naturelles et en génie du Canada, et le Fonds de recherche du Québec - Nature et technologie. Ce travail est une contribution au programme de recherche de Québec-Océan.

AVANT-PROPOS

Ce mémoire a été réalisé dans le cadre d'une maîtrise en océanographie à l'Institut des sciences de la mer de Rimouski (ISMER) débutée en septembre 2018 sous la direction de Michel Gosselin et la codirection de Michel Starr. Le mémoire traite d'une étude en mésocosmes qui a eu lieu à l'été 2018 à la station aquicole de l'ISMER. Tous les travaux d'échantillonnage, d'analyses et de rédaction ont été effectués à Rimouski, territoire ancestral des Premières Nations Wolastoqiyik Wahsipekuk et Mi'kmaq.

L'expérience en mésocosmes est une constituante du 3^{e} volet du Réseau d'observation et de recherche sur la santé de l'écosystème du Saint-Laurent (St. Lawrence ECOsystem Health Research and Observation NETwork - SECO.Net) qui porte sur l'impact de l'eutrophisation sur l'écosystème. Ma participation au projet a débuté en aidant à la préparation et à l'entretien des mésocosmes. Avec l'aide de Constance Duffaud, j'ai participé à l'enrichissement des mésocosmes en nutriments et estimé les vitesses du chute des pigments, du pico- et du nanophytoplancton, et des particules exopolymériques transparentes à partir de colonnes de sédimentation (SetCol). J'ai également déterminé la composition taxonomique du phytoplancton. D'autres membres de l'équipe ont prélevé des échantillons dans les mésocosmes pour la détermination des nutriments, du phosphore organique particulaire et de la silice biogénique, de l'azote organique particulaire et des pigments. Avec l'appui de mes directeurs, j'ai compilé les données, produit les figures et réalisé les tests statistiques. L'interprétation des résultats s'est faite lors de rencontres hebdomadaires avec mes directeurs puis j'ai rédigé le texte. Catherine Lalande a corrigé le mémoire au fur et à mesure puis mes directeurs ont corrigé la version finale.

Ce mémoire est composé d'une introduction générale en français suivi, d'un chapitre central rédigé en anglais sous la forme d'un article scientifique et d'une conclusion générale en français. La rédaction de l'article en anglais a été adoptée à des fins de formation personnelle et de publication éventuelle. L'article sera soumis pour publication dans une revue avec comité de lecture au cours des prochains mois.

Le projet a été présenté sous forme d'une affiche aux réunions scientifiques annuelles de Québec-Océan en 2018 à Rivière-du-Loup et en 2021 en présentation virtuelle. Le prix de la meilleure affiche a été attribué à la présentation de 2021. Une présentation des résultats préliminaires a été faite lors d'un atelier SECO.Net qui a eu lieu à l'ISMER en février 2019. Le séminaire de maîtrise a été présenté dans le cadre d'un webinaire Québec-Océan en décembre 2020 (peut être consulté à l'adresse suivante : https://www.youtube.com/watch?v=WfLrl8aHcc&t=2213s&ab_channel=Qu%C3%A9bec-Oc%C3%A9an). En raison de la pandémie de Covid-19, la présentation des résultats de mon étude qui devait avoir lieu au congrès de l'Acfas à l'Université de Sherbrooke en mai 2020 a été reportée en mai 2021.

RÉSUMÉ

La libération de nutriments azotés provenant de l'agriculture et des eaux usées favorise l'eutrophisation des eaux côtières à travers le monde. L'estuaire maritime du Saint-Laurent montrant des signes d'eutrophisation, une expérience en mésocosmes a été menée durant l'été 2018 afin de déterminer l'impact des variations des apports fluviaux en nutriments azotés sur ce milieu marin. Quatre traitements nutritifs ont été appliqués en début d'expérience afin de recréer : 1) la remontée d'eau à la tête de l'estuaire maritime (contrôle), 2) la rencontre des eaux de remontées et fluviales (+N), 3) cette même rencontre mais avec une plus grande proportion d'urée (+Urée) et 4) une réduction de 50 % des apports fluviaux azotés (–N). La composition des communautés microbiennes et leurs flux verticaux ont été caractérisés pour chaque traitement. Dans tous les traitements, les nutriments ont été consommés en moins de trois jours. Une concentration plus élevée de nutriments azotés a mené à une biomasse carbonée phytoplanctonique et une concentration de particules exopolymériques transparentes plus importantes. La diatomée centrale *Skeletonema costatum* est l'espèce qui a dominé dans tous les traitements. La communauté microbienne a montré une préférence pour le nitrate par rapport à l'urée sauf dans le traitement +Urée où elle a montré une préférence similaire pour le nitrate et l'urée. Les vitesses de chute des particules ont été semblables entre le contrôle et les traitements +N et +Urée, mais le rapport plus élevé entre le silicium dissous et le nitrate dans le traitement –N a favorisé la silicification des diatomées qui a conduit à des vitesses de chute accrues. Les flux verticaux en carbone s'en sont trouvés augmentés de 45 % dans le traitement –N (~ 392 mg C m^{-2} j^{-1}) par rapport aux autres traitements (~ 270, 280 et 253 mg C m^{-2} j^{-1} pour le contrôle, +N et +Urée, respectivement). Il est difficile, à partir de cette étude, de prédire si une réduction en nutriments azotés en aval de la ville de Québec permettrait de réduire l'eutrophisation dans l'estuaire maritime du Saint-Laurent. Ces résultats offrent toutefois des valeurs de vitesses de chute des particules microbiennes isolées de facteurs externes tels que le macrozooplancton et la turbulence, les rendant utiles pour de futurs modèles biogéochimiques.

Mots clés : azote, estuaire du Saint-Laurent, eutrophisation côtière, flux verticaux en carbone, nutriments anthropiques, particules exopolymériques transparentes, phytoplancton, silicification, *Skeletonema costatum*, urée

ABSTRACT

Releases of nitrogenous nutrients associated with agriculture and wastewater treatment promote eutrophication in coastal waters around the world. As the Lower Estuary of St. Lawrence shows early signs of eutrophication, a mesocosm experiment was conducted to determine the impact of variations in river inputs of nitrogenous nutrients on this marine environment. Four treatments were applied at the start of the experiment in order to recreate: 1) the upwelling waters at the head of the Lower Estuary (control), 2) a mix of upwelled and riverine water (+N), 3) the same mix of upwelled and riverine waters with a greater proportion of urea in the total nitrogenous nutrient (+Urea) and 4) waters with a 50% reduction in nitrogenous riverine inputs (–N). The composition and vertical fluxes of the microbial communities were characterized under these four scenarios. In all treatments, nutrients were consumed within three days. A higher concentration of nitrogenous nutrients led to a higher phytoplankton carbon biomass and concentration of transparent exopolymeric particles. The centric diatom *Skeletonema costatum* dominated in all treatments. The microbial community showed a preference for nitrate in all treatments, but showed a similar preference for nitrate and urea in the +Urea treatment. Particle sinking velocities were similar between the control and the +N and +Urea treatments, but the higher dissolved silicon:nitrate ratio in the –N treatment favoured silicification of the diatoms, leading to increased sinking speeds. The vertical carbon fluxes were increased by more than 45% in the –N treatment (~ 392 mg C m^{-2} d^{-1}) compared to the other treatments (~ 270, 280 and 253 mg C m^{-2} d^{-1} in the control, +N and +Urea, respectively). It is difficult to predict whether a reduction in nitrogenous nutrients downstream from Quebec City would reduce eutrophication in the Lower St. Lawrence Estuary. However, these results provide values for the sinking velocities of microbial particles isolated from external factors such as macrozooplankton and turbulence, making them useful for future biogeochemical models.

Keywords: anthropogenic nutrients, carbon sinking flux, coastal eutrophication, nitrogen, phytoplankton, silicification, *Skeletonema costatum*, St. Lawrence Estuary, transparent exopolymeric particles, urea

TABLE DES MATIÈRES

LISTE DES TABLEAUX

LISTE DES FIGURES

INTRODUCTION GÉNÉRALE

ARTICLE SCIENTIFIQUE

LISTE DES ABRÉVIATIONS, DES SIGLESET DES ACRONYMES

BSi Silice biogénique (*Biogenic silica*)

B_s Échantillon de la section inférieure de la colonne de sédimentation

B_t Échantillon témoin à l'extérieur de la colonne de sédimentation

C_f Concentration finale (*Finale concentration*)

CH_4N_2O Urée (*Urea*)

chl *a* Chlorophylle *a* (*Chlorophyll* a)

KNO_3 Nitrate de potassium (*Potassium nitrate*)

KH_2PO_4 Phosphate de potassium (*Potassium phosphate*)

K_s Constante de demi-saturation (*Half-saturation constant*)

$Na_2SiO_3 \bullet 5H_2O$ Métasilicate de sodium (*Sodium metasilicate*)

NH_4 Ammonium

NO_2 Nitrite

NO_3 Nitrate

PO_4 Phosphate

PON Azote organique particulaire (*Particulate organic nitrogen*)

POP Phosphore organique particulaire (*Particulate organic phosphorus*)

RPI Indice de préférence relative (*Relative preference index*)

SECO.Net Réseau d'observation et de recherche sur la santé de l'écosystème du Saint-Laurent (*St. Lawrence ECOsystem Health Research and Observation NETwork*)

SETCOL Colonne de sédimentation (*SETtling COLumn*)

$Si(OH)_4$ Acide silicique

TDN Azote dissous total (*Total dissolved nitrogen*)

TEP Particules exopolymériques transparentes (*Transparent exopolymeric particles)*

INTRODUCTION GÉNÉRALE

Eutrophisation estuarienne

L'accroissement démographique et l'intensification des activités agricoles augmentent la quantité de nutriments qui se déchargent dans les milieux aquatiques (Glibert et al. 2005). L'apport croissant de nutriments, tels le phosphore et l'azote, est responsable de l'eutrophisation des milieux marins côtiers (Pinckney et al. 2001, Rabalais et al. 2009) (Figure 1). Une plus forte disponibilité des nutriments provoque une croissance accrue du phytoplancton, parfois toxique, dans les eaux de surface (Van Meerssche et al. 2018). Si la production phytoplanctonique excède ce que le milieu peut absorber, il en résulte un excès de matière organique particulaire (Rabalais et al. 2009). Cette matière organique particulaire sédimente et est décomposée sous la pycnocline entraînant la déplétion de l'oxygène dissous et l'acidification du milieu, rendant l'environnement hostile à la survie de nombreuses espèces benthiques (Cloern 2001, Rabalais et al. 2009, Gilbert et al. 2010, Carstensen & Duarte 2019). Les zones à hypoxiques peuvent être temporaires et disparaître, soit par un mélange saisonnier des masses d'eaux ou par des efforts législatifs réduisant les apports en nutriments anthropiques, ou encore s'installer de façon permanente (Diaz & Rosenberg 2008).

Au Québec, des interventions d'assainissement et des mesures réglementaires ont été mises en place depuis la fin des années 1970 afin de réduire les apports de phosphore dans l'eau douce et ainsi contrôler l'eutrophisation dans les lacs et les rivières, milieux où le phosphore est habituellement limitant (Gilbert et al. 2007). Toutefois, contrairement aux ventes d'engrais phosphatés qui ont diminué au milieu des années 1980, celles d'engrais azotées ont continué à progresser (Gilbert et al. 2007, Hudon et al. 2018, IFA 2020). Ces changements ont pour effet d'augmenter l'azote dissous par rapport au phosphore dissous (ratio N:P) dans les eaux du fleuve Saint-Laurent qui s'écoulent ensuite vers les eaux de

surface de l'estuaire maritime. Les affluents du Saint-Laurent drainant des terres agricoles apportent entre 20 et 27% de l'azote et du phosphore respectivement retrouvés à l'embouchure de l'estuaire fluvial. Les nutriments provenant de sources municipales comptent pour environ 6%,autant pour l'azote que pour le phosphore. La moyenne annuelle du ratio molaire N:P mesurée à l'embouchure de l'estuaire fluvial est d'environ 50 (Hudon et al. 2017). Dans la zone de transition entre l'eau douce et l'eau salée du Saint-Laurent, le débit important et la faible profondeur créent une zone très turbide où la production primaire est limitée par la lumière (Vincent et al. 1994). Les organismes hétérotrophes y reminéralisent la matière organique particulaire sous forme de nutriments azotés et phosphorés. Les nutriments nouveaux et régénérés provenant de l'estuaire fluvial et moyen seraient finalement principalement consommés dans l'estuaire maritime (Cyr et al. 2015).

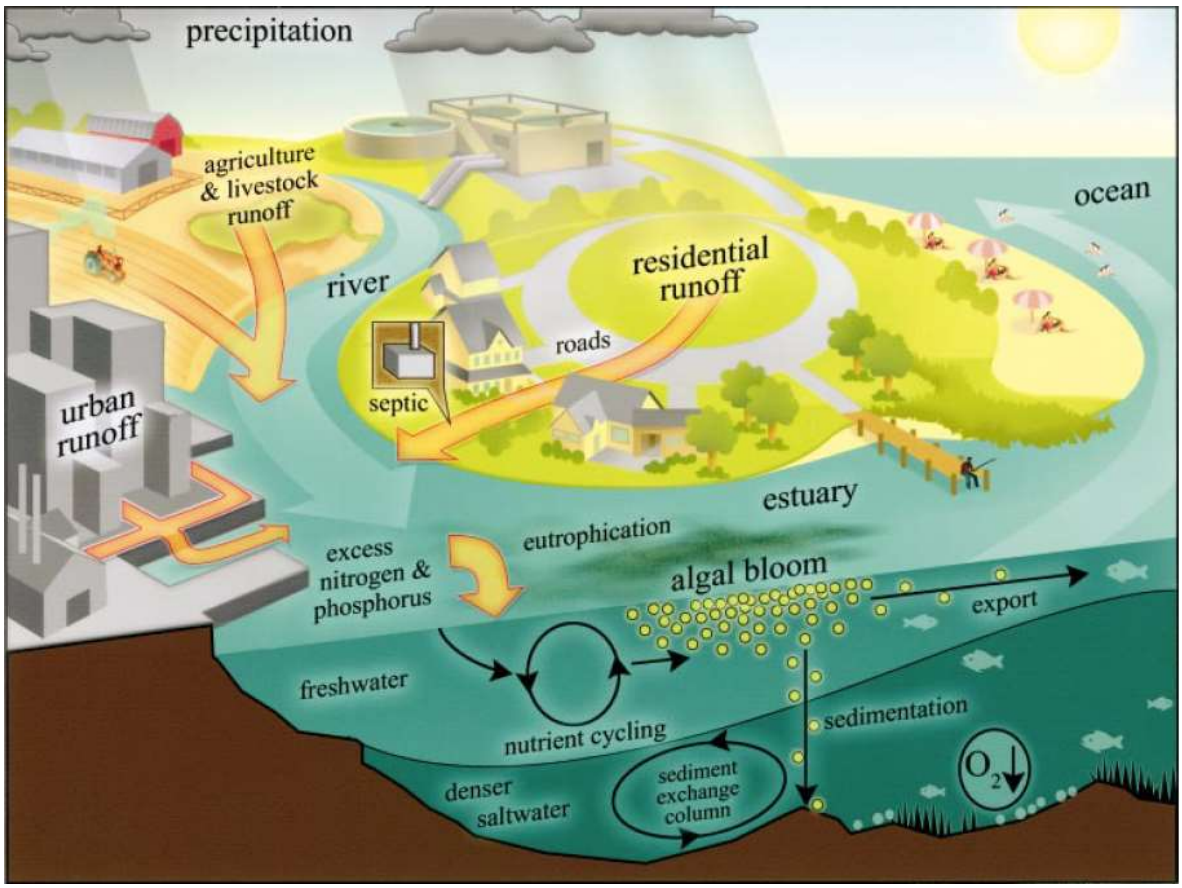

Figure 1. Diagramme conceptuel de l'eutrophisation côtière en milieu estuarien (tiré de Paerl et al. 2006)

En milieu marin, l'azote est généralement le nutriment qui limite la production primaire (Hecky & Kilham 1988, Pinckney et al. 2001, Villeneuve 2020). En milieu côtier, l'augmentation des apports en azote dissous accroît la prolifération du phytoplancton et le changement du ratio N:P des apports en nutriments influence la composition taxonomique de la communauté phytoplanctonique (Smith 1990, Lagus et al. 2004, Paerl et al. 2004, Howarth et al. 2006, Pinckney et al. 2020). Une diminution du rapport N:P de l'eau provoquerait une augmentation de la prolifération des cyanobactéries toxiques dans la mer Baltique à la fin de l'été (Niemi 1979, Granéli et al. 1990). À l'inverse, une augmentation du rapport N:P de l'eau peut mener à une augmentation de l'abondance des espèces mixotrophes comme le chrysophyte *Uroglena* spp., mais aussi d'autres espèces dont certaines pourraient être nuisibles, comme le prymnésiophyte *Chrysochromulina polylepis* dans la mer de l'Archipel, au nord de la mer Baltique (Lagus et al. 2004). Dans les eaux de surface (0 à 25 m) de l'estuaire maritime du Saint-Laurent, les concentrations en phosphate restent similaires à travers les saisons (~ 1 μmol L^{-1}) alors que celles en nitrate varient beaucoup plus avec un minimum autour de 5 μmol L^{-1} à l'été et un maximum d'environ 15 μmol L^{-1} au printemps (Villeneuve 2020). Le rapport molaire N:P y varie entre 0,5 et 7 ce qui se situe bien en dessous du rapport de Redfield de 16, signifiant une forte limitation en azote dans ce milieu (Redfield et al. 1963, Villeneuve 2020).

Dans les eaux oligotrophes et mésotrophes, le rapport d'approvisionnement N:P ou N:Si en plus de la concentration absolue en nutriments structurent la communauté phytoplanctonique. En effet, lors d'une expérience de compétition pour les nutriments entre deux espèces de diatomées centrales, Lagus et al. (2004) ont montré que *Chaetoceros swighamii* domine à des concentrations faibles en nutriments et des ratios N:P élevés, alors que *Skeletonema costatum* est favorisée à des concentrations élevées et rapports N:P plus faibles.

Si les engrais azotés, tels ceux contenant du nitrate, de l'azote ammoniacal et de l'urée, continuent à être de plus en utilisés en agriculture et que les stations d'épuration municipales ne retirent pas l'azote dissous des eaux usées, cela pourrait favoriser l'eutrophisation côtière dans l'estuaire maritime du Saint-Laurent (Gilbert et al. 2007).

Hypoxie à la tête du chenal Laurentien

Le chenal Laurentien débute au seuil entre l'estuaire moyen et l'estuaire maritime du Saint-Laurent au niveau de Tadoussac (Figure 2).Ce chenal d'une profondeur comprise entre 200 et 550 m s'étend sur 1 240 km jusqu'à l'Atlantique Nord en passant par le golfe du Saint-Laurent. Les courants de l'Atlantique Nord et du Labrador pénètrent dans le chenal, circulent en profondeur et remontent en surface à l'approche du seuil. En surface, les eaux provenant de l'estuaire fluvial s'écoulent vers la partie maritime et rencontrent celles du chenal tout juste passé le seuil (Saucier et al. 2003). Des études dans l'estuaire maritime du Saint-Laurent démontrent que certaines zones profondes, principalement à la tête du chenal Laurentien, présentent des teneurs en oxygène inférieures au seuil d'hypoxie (< 62 µmoles O_2 L^{-1}) (Gilbert et al. 2005, Thibodeau et al. 2006). Ces concentrations trop faibles pour le maintien de la vie de nombreuses espèces benthiques importantes pour les pêcheries canadiennes semblent, depuis la fin des années 1980, persister à l'année longue (Gilbert et al. 2005) en plus d'entraîner l'acidification des eaux profondes de l'estuaire maritime du Saint-Laurent (Mucci et al. 2011).

Selon Jutras et al. (2020a), les causes de la baisse d'oxygène dans l'estuaire maritime ont varié au cours des cinquante dernières années. Entre les années 1970 et la fin des années 1990, le déclin était principalement attribuable aux changements biogéochimiques dus à une augmentation de l'utilisation microbienne de l'oxygène en réponse à des températures plus chaudes et à l'eutrophisation et à des concentrations d'oxygène plus faibles dans les deux principales masses d'eau alimentant le système (c.-à-d., les eaux du courant du Labrador et les eaux centrales de l'Atlantique Nord) (Jutras et al. 2020a). L'eutrophisation est un mécanisme par lequel les apports de nutriments et de matière organique provenant des activités urbaines et agricoles favorisent la prolifération d'algues, qui sont décomposées par des bactéries qui consomment de l'oxygène dans les eaux profondes (Benoit et al.2006, Thibodeau et al.2006, Lehmann et al. 2009). Depuis les années 2000 à aujourd'hui, la diminution était principalement attribuable aux changements de circulation dans l'ouest de l'Atlantique Nord associés à une réduction de la quantité d'eaux du Labrador alimentant le système (Lehmann et al.2009, Claret et al.2018, Jutras et

al. 2020a). Étant donné que les changements de circulation dans l'ouest de l'Atlantique Nord sont liés au changement climatique, il est difficile de proposer une législation locale pour s'attaquer à cette cause du déclin de l'oxygène dans l'estuaire maritime du Saint-Laurent. Par conséquent, il devient essentiel de se concentrer sur les causes locales telles que l'augmentation des apports fluviaux de nutriments provenant des activités urbaines et agricoles pour résoudre ce problème.

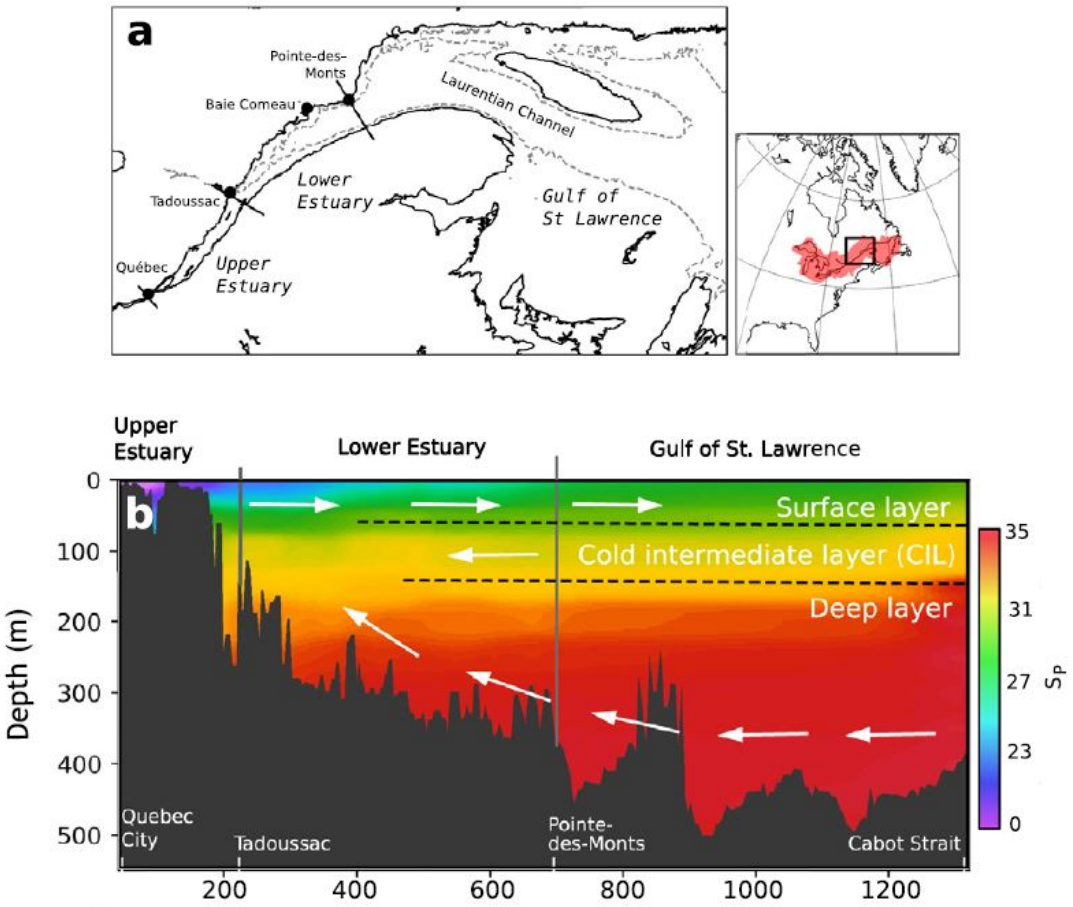

Figure 2. Bassin central de l'estuaire maritime du Saint-Laurent (Lower Estuary) avec l'estuaire moyen (Upper Estuary) en amont et le golfe du Saint-Laurent en aval (Gulf of St. Lawrence). a) le chenal Laurentien (Laurentian Channel) est tracé par la ligne point (tiré de Jutras et al. 2020b)

Voies de transfert de la matière organique : flux verticaux

Le flux vertical de la matière organique dépend de la composition, la quantité et la vitesse de chute de cette matière (Eppley & Peterson 1979, Bienfang et al. 1983). La production primaire par les organismes unicellulaires autotrophes qui constituent le phytoplancton se fait dans la zone euphotique (Figure 3). Les particules phytoplanctoniques sédimentent dans les couches inférieures sous forme de cellules entières, de pelotes fécales et d'agrégats et sont décomposées par les bactéries hétérotrophes ce qui y augmente la demande en oxygène (Gilbert et al. 2007), puisque que l'oxygène est utilisé pour l'oxydation de la matière organique. Les particules exopolymériques transparentes, exsudées par le phytoplancton et les bactéries, sédimentent relativement lentement et sont davantage photooxydées en surface ou utilisées par les bactéries et certains flagellés hétérotrophes. En milieu aquatique, la vitesse de chute des particules est régie par la balance entre l'accélération gravitationnelle de la particule et la traînée agissant sur celle-ci via sa surface et le frottement du fluide selon la loi de Stokes (Lerman et al. 1974). Ainsi, la taille et la densité de la particule sont des paramètres clés. Plusieurs facteurs peuvent cependant faire varier ces paramètres les rendant difficilement intégrables dans la loi de Stokes qui considère les particules comme lisses et sphériques (Laurenceau-Cornec et al. 2019). La mortalité des cellules, soit par déficience en nutriments (Bienfang et al. 1982, 1983), par infection virale (Fuhrman 1999) ou par broutage (Michaels & Silver 1988), peut influencer la flottabilité des particules microbiennes. La turbulence (Pesant et al. 2002) et l'abondance des cellules (Jackson 1990) peuvent accentuer l'agrégation, influençant ainsi la taille et la densité des particules. En milieu estuarien, les particules exopolymériques transparentes sont abondantes surtout suivant des périodes d'efflorescences (Annane et al. 2015). Leur présence favorise l'agrégation des particules et joue un rôle prépondérant sur les flux (Passow et al. 2001, Azetsu-Scott & Passow 2004). Un accroissement de nutriments azotés en surface favorise les efflorescences dominées par les diatomées (Plourde & Therriault 2004), soit de relativement grosses et denses cellules productrices de particules exopolymériques transparentes (Passow et al. 1994). Différentes mesures de flux verticaux ont été faites dans le golfe du Saint-Laurent pendant le programme canadien

JGOFS au début des années 1990. À l'aide de pièges à particules disposés à différentes stations et profondeurs, des flux de carbone ont été estimés entre 48 et 257 mg C m^{-2} j^{-1} en juillet 1993 (Romero et al. 2000).

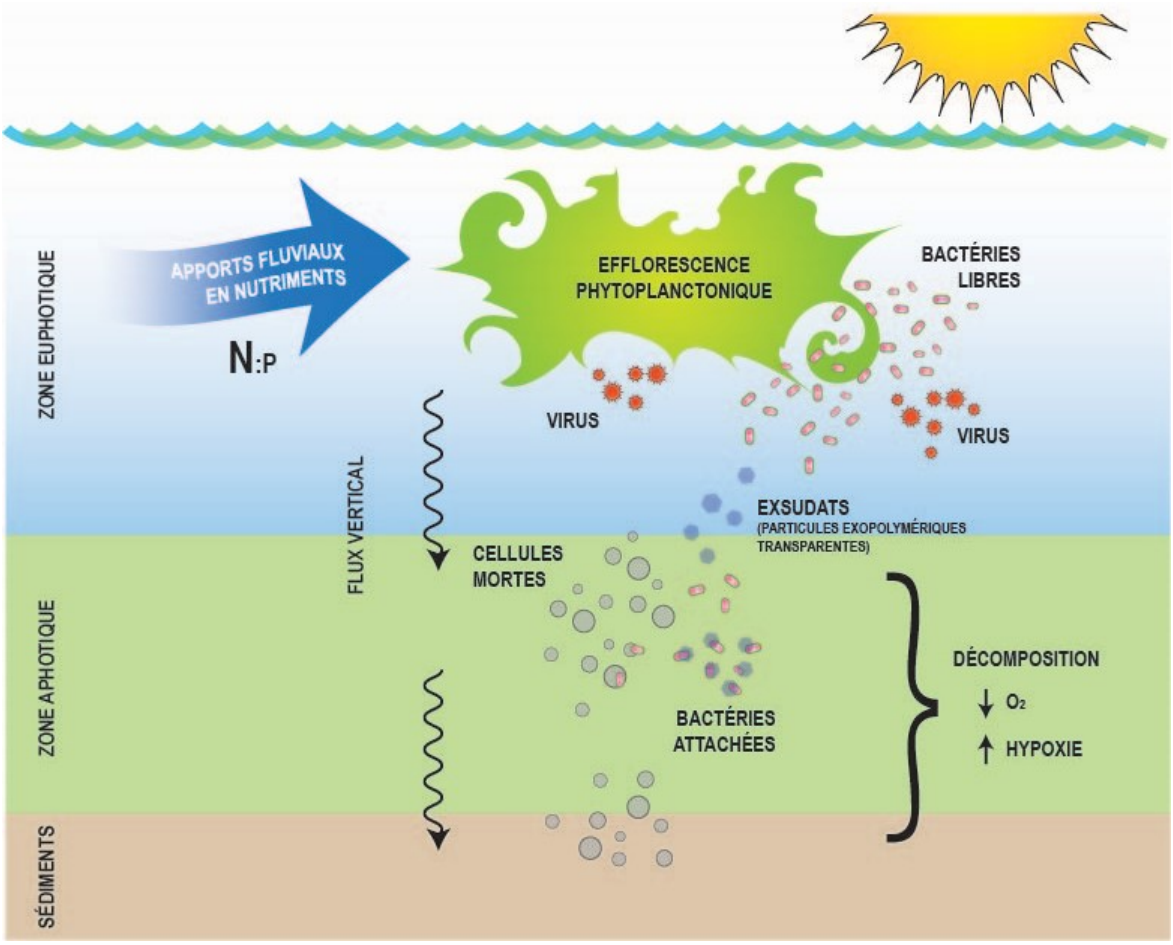

Figure 3. Schéma conceptuel de l'influence des apports fluviaux en nutriments sur les flux verticaux et la demande en oxygène (adapté de Sarmiento & Gruber 2006)

Variation des ratios de nutriments et ses effets sur les communautés microbiennes

En milieu marin, la croissance du phytoplancton est potentiellement limitée par les apports en macronutriments (azote, silicium ou phosphore) ou en micronutriments (fer, cobalt ou vitamine B_{12} [cobalamine]) (Hecky & Kilham 1988, Sañudo-Wilhelmy et al.

2006). Le système marin du Saint-Laurent comme l'Atlantique Nord tend à être limité en azote dissous (Howarth et al. 1996).

La stœchiométrie et la spéciation de ces éléments influencent la structure de la communauté phytoplanctonique (Tilman 1982, Tilman et al. 1982, Pinckney et al. 2001). L'issue des interactions compétitives entre les espèces pour l'acquisition des nutriments à l'intérieur des communautés phytoplanctoniques peut avoir des implications importantes sur le cycle du carbone, comme par exemple, en influençant la structure trophique et/ou en contrôlant la séquestration du carbone à l'intérieur des océans. Une augmentation du ratio N:P en milieu estuarien peut potentiellement entraîner un changement de population dominée par les cyanobactéries à une population dominée par les chlorophytes et les diatomées (Smith 1990). Paerl et al. (2004) démontrent qu'à la fin des années 1980, dans l'estuaire de la rivière Neuse en Caroline du Nord aux États-Unis, les concentrations en chlorophylle *a*, un indicateur de biomasse phytoplanctonique, ont diminué suite à une réduction du phosphate dans l'eau. Au cours des années qui ont suivi, la biomasse phytoplanctonique a augmenté dans la partie marine de l'estuaire avec des efflorescences dominées par des dinoflagellés, des cryptomonades et des diatomées. Certaines espèces sont aussi connues pour développer une plus forte toxicité quand exposées à des ratios N:P plus élevés (Anderson et al. 2008). Des efforts de réductions en phosphate, non accompagnés de réduction en azote dans un bassin versant d'estuaire peuvent ainsi provoquer l'eutrophisation et les efflorescences toxiques dans l'écosystème marin en aval.

Un changement de communauté peut aussi survenir en variant les proportions inorganiques et organiques de l'azote. L'urée, une source d'azote organique, constitue plus de la moitié de l'azote utilisé en engraisen plus d'être aussi rejeté par les eaux urbaines (Glibert et al. 2006). Non seulement l'urée favorise la croissance des plantes, cet engrais est plus stable que le nitrate d'ammonium qui est utilisé comme source d'engrais en agriculture. Ce dernier peut être très explosif comme en témoigne la catastrophe dans le port de Beyrouth en août 2020. Pour l'épandage agricole, l'urée est souvent enfouie et appliquée avant une pluie, la rendant sensible au lessivage (Ziadi et al. 2007). Selon les données de l'association internationale des engrais (*International Fertilizer Association*), l'utilisation de

l'urée en agriculture était d'environ 40 milles tonnes au Canada en 1973. Cette valeur a continuellement augmenté pour atteindre 1 355 milles tonnes en 2018 (IFA 2020) (Figure 4). Cette forme d'azote est consommée de manière préférentielle par rapport au nitrate par plusieurs espèces phytoplanctoniques, dont *Skeletonema costatum* (Huang et al. 2020), une diatomée abondante dans l'estuaire du Saint-Laurent. Toutefois une augmentation de l'urée dans le milieu marin favorise la présence de dinoflagellés toxiques (Glibert et al. 2006).

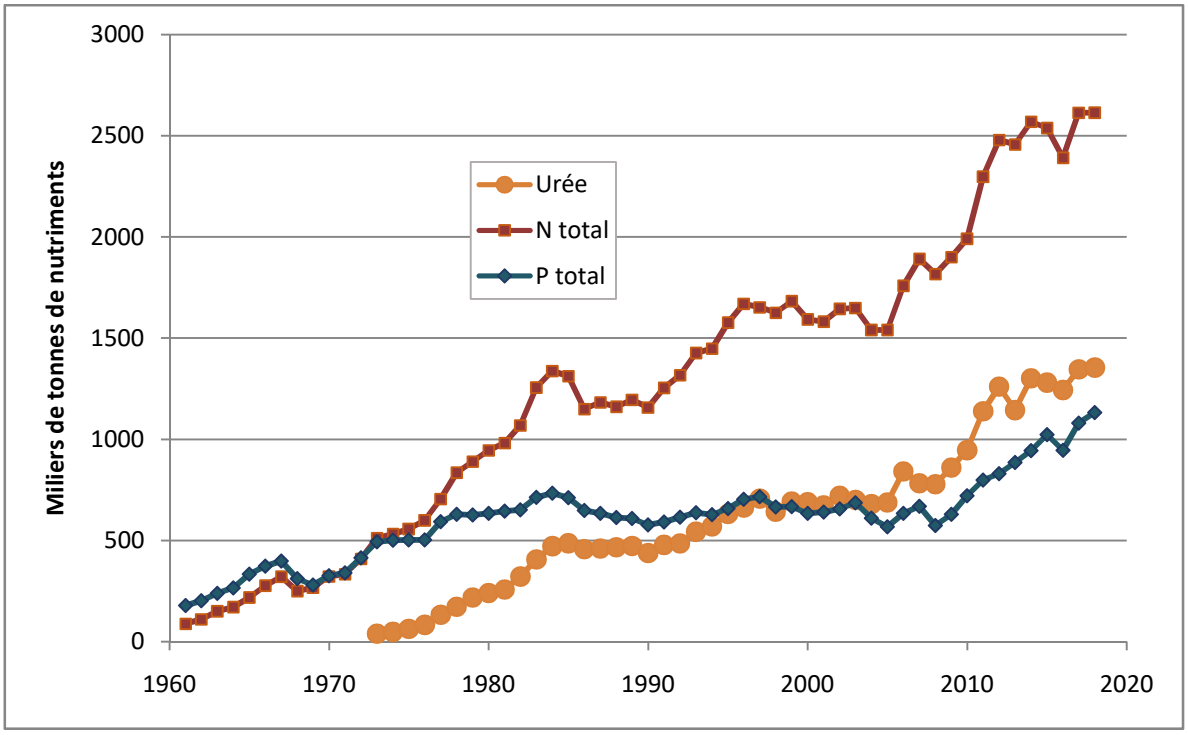

Figure 4. Évolution de l'utilisation de l'azote total, du phosphore total et de l'urée comme engrais agricoles au Canada de 1961 à 2018 (Adaptée de IFA 2020)

Le phytoplancton, les bactéries libres et attachées aux particules sont des composantes planctoniques dont l'abondance et l'activité varient en fonction des nutriments (Figure 3). La production des bactéries libres dépend, entre autres, des concentrations en nutriments et de l'abondance du phytoplancton qui exsude du carbone organique dissous. Une plus grande concentration de particules organiques favorisent la présence de bactéries

attachées (Barrera-Alba et al. 2009, Lapoussière et al. 2011). Ainsi, un changement dans les ratios de nutriments a un effet sur les structures des communautés microbiennes.

Des données pour la modélisation dans le Saint-Laurent

L'évolution rapide des changements liés au réchauffement des océans et à l'eutrophisation côtière appelle à la modélisation. Les simulations fiables dépendent des données prises sur le terrain ou provenant d'expériences en milieux contrôlés. La population humaine et l'utilisation d'engrais azotés sur les bassins versants du Saint-Laurent étant en croissance, il importe de pouvoir projeter les effets des apports de nutriments à moyen et long terme. Dans une étude de modélisation numérique, Benoit et al. (2006) ont testé dans quelle mesure l'hypoxie dans le chenal Laurentien pourrait être associée à une plus grande demande en oxygène dans la colonne d'eau et les sédiments en raison de l'eutrophisation. En se basant sur des données *in situ*, les auteurs conclurent que leur modèle surestime la consommation d'oxygène par les sédiments au niveau de l'estuaire maritime. Benoît et al. (2006) suggèrent que la consommation d'oxygène dans la colonne d'eau pourrait être plus importante que prévue, mais déplore un manque de données pour la région étudiée.

Pour tester la sensibilité de l’estuaire maritime du Saint-Laurent aux perturbations environnementales, Jutras et al. (2020b) ont construit un modèle à boîte pour cet écosystème. Ce modèle focalise sur la stratification de l’estuaire maritime durant la période libre de glace et est contraint par des données recueillies sur le terrain au cours de la dernière décennie (p. ex., salinité, température, nutriments et oxygène dissous). Le modèle démontre que non seulement l'eutrophisation serait due à une augmentation des apports fluviaux, mais aussi à une variation dans le volume des courants entrant dans le golfe du Saint-Laurent depuis l'Atlantique Nord-Ouest. Il importe donc de tester les effets des apports fluviaux en nutriments azotés sur la dynamique microbienne afin d'obtenir des valeurs fiables à inclure dans des modèles numériques. Les données de flux verticaux du carbone biogène représentent une composante importante pour mesurer si l'eutrophisation participe à la désoxygénation des eaux profondes de l'estuaire maritime du Saint-Laurent.

Objectifs et hypothèses

C'est dans la perspective d'étudier le phénomène d'eutrophisation dans l'estuaire du Saint-Laurent que le Réseau d'observation et de recherche sur la santé de l'écosystème du Saint-Laurent (*St. Lawrence ECOsystem Health Research and Observation NETwork* - SECO.Net) a été créé en 2017. La présente étude s'inscrit dans le volet expérimental de ce réseau de recherche.

L'objectif général de ce projet de maîtrise est de déterminer expérimentalement l'impact d'une variation des apports fluviaux en nutriments azotés sur les flux verticaux des particules microbiennes (phytoplanctonique et bactérienne) dans l'estuaire maritime du Saint-Laurent. Ce travail permettra de tester à la fois les effets de la concentration et de la composition des nutriments azotés sur la dynamique des premiers échelons planctoniques. En mésocosmes, trois environnements réalistes, ont été recréés : un actuel (+N) simulant la rencontre entre les eaux de remontée de l'estuaire maritime et celles de l'estuaire fluvial du Saint-Laurent; un futuriste (+Urée) avec un apport plus important en urée; et un de réduction (–N) où les apports fluviaux en nitrate sont diminués de 50% grâce à, par exemple, une volonté gouvernementale de réduire l'eutrophisation. L'hypothèse générale est que les apports fluviaux en nutriments azotés, principalement organiques, augmentent les flux descendants de particules microbiennes dans l'estuaire maritime.

Le premier objectif spécifique est de caractériser les communautés microbiennes d'une efflorescence phytoplanctonique en mesurant les concentrations de matière particulaire et de pigments, en dénombrant les abondances cellulaires et en notant la composition taxonomique selon différentes concentrations de nutriments azotés. L'hypothèse à tester est qu'une concentration plus élevée en nutriments azotés favorise une communauté microbienne abondante et qu'une plus grande proportion d'urée favorise la croissance d'espèces phytoplanctoniques potentiellement toxiques.

Le second objectif spécifique est de quantifier les flux verticaux pendant une efflorescence phytoplanctonique selon les communautés et les différentes concentrations en azote. L'hypothèse à tester est qu'une variation dans la biomasse et la composition des communautés fait varier les flux descendants. Comme une plus forte concentration de

nutriments azotés devrait faire augmenter la biomasse phytoplanctonique, les flux descendants de matière organique devraient augmenter sous l'effet d'un enrichissement en azote.

Cette étude expérimentale sur l'effet des apports en nutriments azotés sur la composition et les flux descendants des communautés microbiennes fournira des informations essentielles pour mieux comprendre l'impact de l'eutrophisation côtière dans l'estuaire maritime du Saint-Laurent.

EFFECTS OF RIVERINE NUTRIENT INPUTS ON THE DOWNWARD FLUXES OF MICROBIAL PARTICLES IN THE ST. LAWRENCE ESTUARY

1 INTRODUCTION

Population growth and agricultural development increase the amount of nutrients that are released into aquatic environments (Gilbert et al. 2005, Smith & Schindler 2009). The enhanced input of nutrients, such as phosphorus and nitrogen, causes the eutrophication of coastal marine environments (Pinckney et al. 2001, Rabalais et al. 2009). High nutrient availability favour growth conditions for algal blooms that may sometimes be harmful (Pinckney et al. 2001, Van Meerssche et al. 2018). Massive phytoplankton production may enhance sedimentation and subsequent decomposition of particulate organic matter under the pycnocline, potentially leading to the depletion of dissolved oxygen and ocean acidification, making the environment hostile to the survival of demersal and benthic species (Cloern 2001, Rabalais et al. 2009, Gilbert et al. 2010). Hypoxic zones may be short-lived following the seasonal mixing of water masses reintroducing oxygen at depth, may disappear following legislative efforts to reduce the input of anthropogenic nutrients, or may become permanent (Diaz & Rosenberg 2008).

The ongoing worldwide coastal eutrophication problem has frequently been reported. In 1999, the National Oceanic and Atmospheric Administration reported that in the United States, 84 out of 122 estuaries studied were presenting moderate to high eutrophication symptoms such as depleted dissolved oxygen and harmful algal blooms (Bricker et al. 1999). The Baltic Sea also increasingly experienced severe eutrophication due to high anthropogenic nutrients loads (Carstensen et al. 2014), similar to the Gulf of Mexico and

eastern Chinese coastal waters (Cai et al. 2011, Jiang et al. 2018). Eutrophication is clearly a worldwide issue.

Since the late 1970s, sanitary interventions and regulatory measures have been implemented in Quebec (Canada) to reduce phosphorus domestic, agricultural and industrial inputs into lakes and rivers and reduce eutrophication in these typically phosphorus-limited environments (Gilbert et al. 2007). However, while these regulations led to a decline in phosphate utilization in the mid-1980s, utilization of nitrogenous fertilizers continued to increase (Gilbert et al. 2007, Hudon et al. 2018). Many of this nitrogen fertilizer used in Québec and worldwide is urea-based and found in agriculture products, animal feeds and urban and industrial wastes. Thus, urea contributes to a significant fraction of the total dissolved nitrogen (TDN = NO_3 + NO_2 + NH_4 + N-urea) found in coastal waters, potentially promoting the growth of harmful algal bloom species (Glibert et al. 2006). The increasing use of nitrogenous fertilizers increases the proportion of dissolved nitrogen to dissolved phosphorus (N:P ratio) in the Upper St. Lawrence Estuary, and eventually in the Lower Estuary (Hudon et al. 2018, Villeneuve 2020). As nitrogen generally limits algal growth in marine environments (Pinckney et al. 2001), an increase in nitrogen inputs usually intensifies the proliferation of phytoplankton and influences its specific composition (Smith 1990, Paerl et al. 2004). A higher N:P ratio also promotes the growth of harmful algal species (Glibert 2020). A sustained agriculture-based utilization of nitrogenous fertilizers containing nitrate, ammoniacal nitrogen, and urea in agriculture, along with an absence of municipal wastewater treatment to remove dissolved nitrogen, may promote coastal eutrophication in the Lower St. Lawrence Estuary (Gilbert et al. 2007).

In the deep waters of the Lower St. Lawrence Estuary lays the Laurentian Channel, a deep submarine valley (200-550 m depth) extending over 1,240 km from its head at the mouth of the Saguenay Fjord to Cabot Strait in the Gulf of St. Lawrence. The North Atlantic and Labrador currents enter the channel, circulate at depth and rise to the surface at

the sill at the mouth of the Saguenay Fjord. Surface waters from the Upper Estuary flow towards the Lower Estuary and meet upwelled channel waters just past the sill (Saucier et al. 2003). Dissolved oxygen levels below the hypoxia threshold (<63 μmol O_2 L^{-1}) are observed in deep areas of the Lower St. Lawrence Estuary principally at the head of the Laurentian Channel (Gilbert et al. 2005, Thibodeau et al. 2006). These lowlife-sustaining concentrations of dissolved oxygen for many benthic species important to Canadian fisheries seem to persist throughout the year since the late 1980s (Gilbert et al. 2005).

According to Jutras et al. (2020a), the causes of the oxygen decline in the Lower Estuary varied over the past fifty years. Between the 1970s and the late 1990s, the decline was mainly driven by biogeochemical changes through an increase in microbial oxygen utilization in response to warmer temperatures and eutrophication and lower oxygen concentrations in the two major water masses feeding the system (i.e., the Labrador Current Waters and the North Atlantic Central Waters) (Jutras et al. 2020a). Eutrophication is a mechanism by which nutrient and organic matter inputs from urban and agriculture activities promote algae blooms, which are decomposed by bacteria that consume oxygen in the deep waters (Benoit et al. 2006, Thibodeau et al. 2006, Lehmann et al. 2009). From the 2000s until today, the decrease was mainly driven by circulation changes in the western North Atlantic associated with a reduction in the amount of Labrador waters feeding the system (Lehmann et al. 2009, Claret et al. 2018,Jutras et al. 2020a). Since circulation changes in the western North Atlantic are linked to global climate change, it is difficult to propose local legislation to address this cause of oxygen decline in the Lower St. Lawrence Estuary. Therefore, it becomes essential to focus on local causes such as increased river inputs of nutrients from urban and agricultural activities to address this problem.

In this context, the objective of the present study was to experimentally assess the impact of variations in riverine inputs of nitrogenous nutrients on the composition and vertical downward fluxes of phytoplankton and bacteria in the Lower St. Lawrence Estuary. The first specific objective was to characterize the microbial communities of a

phytoplankton bloom under varying concentrations of nitrogenous nutrients. We hypothesized that a higher concentration of nitrogenous nutrients will result in a more abundant microbial community, and that a greater proportion of urea promotes harmful algal growth. The second specific objective was to quantify the vertical carbon fluxes under different nitrogen concentrations. We hypothesized that a variation in the biomass and composition of the communities influence the downward carbon fluxes. As a higher concentration of nitrogenous nutrients should increase the phytoplankton biomass, the downward fluxes of organic matter should increase under the effect of nitrogen enrichment. This experimental study on the effect of nitrogenous nutrient input on the composition and downward fluxes of the microbial communities will provide critical information to understand better the impact of coastal eutrophication in the Lower St. Lawrence Estuary.

2 MATERIALS AND METHODS

2.1 Experimental design

A mesocosm experiment was conducted during summer 2018 (July 25–August 15) at the Aquaculture station (Pointe-au-Père, Canada) of the Institut des sciences de la mer de Rimouski. On July 25, the Lower St. Lawrence Estuary seawater was collected at 2 m depth from the Rimouski wharf (48º28'39.9"N, 68º31'03.0"W) using an intake pump and transferred to a tanker truck. Collected seawater arrived at the Aquaculture station less than 2 hours after sampling. The seawater added to the mesocosms was first sieved through a 300 µm mesh plankton net to remove the large zooplankton. Using a custom made "octopus" tubing system, seawater was then equally distributed by gravity into 12 cylindrical mesocosms (height: 2.67 m; diameter: 1.4 m) with a conical bottom and a

2 600 L capacity (Aquabiotech Inc., Québec, Canada). The mesocosms, housed in two temperature-controlled shipping containers, are described in detail in Bénard et al. (2018).

Temperature sensors (AQBT-Temperature sensor, accuracy ± 0.2°C) were calibrated and installed on each mesocosm a few days before starting of the experiment. Each mesocosm was sealed with a transparent Plexiglas cover allowing the transmission of 90% of the photosynthetically active radiation (PAR: 400-700 nm), 85-90% of the UVA (315-400 nm), and 50-85% of the UVB (280-315 nm). Seawater (27.2 PSU, as measured with a Guildline model 8400A autosal salinometer) was maintained at a constant temperature of 8°C using a glycol cooling system (Process Technology TTA1.8215). Due to high chlorophyll *a* (chl *a*) concentration on July 25 (~4 µg chl *a* L^{-1}), particulate matter was allowed to sediment for two days. On July 27 and 28 around noon (Eastern Daylight Time), 200 L of water at the bottom of each mesocosm was flushed to avoid remineralization of the sedimented material. In the early afternoon of July 28 (day -1), mesocosm water levels were adjusted and the mixing system (propeller turning at a speed of 10 cm s^{-1}) was turned on to maintain a homogeneous distribution of water characteristics. Nutrient enrichment took place during sunset at 8:00 p.m. At this time, nitrate and silicic acid were almost exhausted with concentrations of 0.05 µM and < 0.1 µM, respectively, while phosphate was still abundant with a value of 1.0 µM.

Four nutrient treatments were applied during this mesocosm experiment (Table 1). The added nutrients were potassium nitrate (KNO_3), N-urea (CH_4N_2O), potassium phosphate (KH_2PO_4**)** and sodium metasilicate ($Na_2SiO_3 \bullet 5H_2O$**).** Each nutrient treatment was performed in triplicate. The control treatment was designed to reproduce the nutrient concentrations in upwelled water from the cold intermediary layer at the head of the Laurentian Channel (final values: NO_3 = 12.0 µM; N-urea = 0.58 µM; ∑N:P = 8.8 at/at; ∑N:Si = 0.90 at/at) based on the climatology estimated from the Rimouski station data of the Atlantic Zone Monitoring Program, 1999-2014 (Department of Fisheries and Oceans Canada; Data archive in Biochem database accessible online at: https://www.dfo-

mpo.gc.ca/science/data-donnees/biochem/index-eng.html). The second treatment (+N) replicated the mixing of surface waters of the St. Lawrence River with the control water (final values: NO_3 = 16.3 µM; N-urea = 0.63 µM; ∑N:P = 13.6 at/at; ∑N:Si = 0.82 at/at). We considered that surface nutrient concentrations near Québec-Lévis were 28 µM for NO_3, 2.4 µM for N-urea, 0.5 µM for PO_4 and 40µM for $Si(OH)_4$ (Villeneuve 2020) and assumed that 27% of riverine surface waters mixed with the upwelled water at the head of the Lower Estuary during summer (Gilbert et al. 2007). The third treatment (+Urea) was similar to the (+N) treatment, but we assumed that N-urea contributes to 33% of the total nitrogen (i.e., N-urea + NO_3) input from the St. Lawrence River (final values: NO_3 = 14.1 µM; N-urea = 1.72 µM; ∑N:P = 13.6 at/at; ∑N:Si = 0.82 at/at). This treatment considered the potential increase in N-urea runoffs due to enhanced utilization of N-urea as a land fertilizer in agriculture in the St. Lawrence Valley. The last treatment (–N) represented a scenario where surface nitrate concentrations in the St. Lawrence River are reduced by 50% due to legislative efforts (final values: NO_3 = 12.5 µM; N-urea = 0.63 µM; ∑N:P = 10.7 at/at; ∑N:Si = 0.64 at/at).

Table 1. Initial nutrient concentrations and ratios for the four treatments of the mesocosm experiment. ∑N = nitrate + N-urea

	Control	**+N**	**+Urea**	**–N**
Nitrate (µM)	12.0	16.3	14.1	12.5
N-urea (µM)	0.58	0.63	1.72	0.63
Phosphate (µM)	1.49	1.29	1.29	1.29
Silicic acid(µM)	14.6	21.4	21.4	21.4
∑N:P (at/at)	8.8	13.6	13.6	10.7
∑N:Si (at/at)	0.90	0.82	0.82	0.64

2.2 Seawater sampling and analysis

From July 29 (day 0), all mesocosms were sampled between 08:00 and 09:00 a.m. Seawater for nutrient, bacteria, picophytoplankton (0.2-2 µm) and nanophytoplankton (2-20 µm) concentration measurements was collected directly from port of the mesocosms located at about 1 m from the bottom. Seawater was also collected in 7 L carboys for the determination of chl *a*, pheopigments, particulate organic nitrogen (PON), particulate organic phosphorus (POP), biogenic silica (BSi), transparent exopolymeric particles (TEP), protist taxonomy, and sinking velocities.

Samples for inorganic nutrient measurements were collected twice a day from day 0 to 8, and every second day from day 10 to 16, whereas urea samples were collected every day throughout the experiment. Seawater subsamples were filtered onto Whatman GF/F filters (nominal porosity of ~0.7 µm) and the filtrates were frozen at -20°C into acid-washed polypropylene tubes for later analysis of NO_3, NO_2, PO_4 and $Si(OH)_4$ with a Bran-Luebbe Autoanalyzer III (AA3) using the colorimetric method adapted from Hansen & Koroleff (1999) and of N-urea, using the spectrophotometric method described in Goeyens et al. (1998). Ammonium (NH_4) concentrations were measured using the fluorometric method of Holmes et al. (1999). The detection limits were 0.03 µM for NO_3, 0.02 µM for NO_2 and NH_4, 0.05 µM for PO_4 and 0.1 µM for $Si(OH)_4$ and N-urea.

For chl *a* and pheopigments determination, daily samples were filtered on Whatman GF/F filters and extracted in 90 % acetone for 18 to 24 h at 4°C in the dark. Concentrations were measured using a Trilogy Com 3 fluorometer following the Parsons et al. (1984) acidification method.

Samples for PON, POP and BSi determination were collected every day during the first 8 days of the experiment and every two days from day 10 to 16. PON and POP samples were filtered onto pre-combusted (450°C for 5h) Whatman GF/F filters. PON was analyzed on a CHN/O/S elemental analyzer Vario MICRO (Elementar) whereas POP was

determined according to the method of Solorzano & Sharp (1980). Samples for BSi determination were filtered onto 0.8 µm Nuclepore polycarbonate membranes and analyzed using the alkaline hydrolysis method of Paasche (1980). The concentrations of particulate material converted into PO_4 and $Si(OH)_4$ were then determined using the above-mentioned nutrient autoanalyzer.

To determine the abundance of picophytoplankton and nanophytoplankton, and heterotrophic nanoflagellates, two subsamples of 4.95 mL were transferred into sterile polypropylene cryovials containing 50 µL glutaraldehyde (Grade I, Sigma, final concentration (C_f) = 0.1%) and kept in the dark for 15 min at room temperature, and then stored at -80°C until analysis by flow cytometry (Marie et al. 1997, Lapoussière et al. 2011). Pico- and nanophytoplankton cells were counted by a CytoFLEX Flow Cytometer (Beckman Coulter) equiped with a blue laser (488 nm) and a red laser (638 nm) using the method described in Marie et al. (2005). Cytograms were interpreted using the CytExpert v2.3 software. As cyanobacteria abundances were low (a mean of ~ 2 cells mL^{-1}) they will not be discussed. For simplicity, the terms picophytoplankton and nanophytoplankton will be used throughout the manuscript to define photosynthetic picoeukaryotes and photosynthetic nanoeukaryotes, respectively.

Heterotrophic flagellate samples were thawed and stained with SYBR Green I (Invitrogen) (Christaki et al. 2011). The CytoFLEX Flow Cytometer counted cells for 10 minutes at a flow rate of 100 µL per minute. The blue laser (488 nm) excited the nucleic acid-bound SYBR Green I and the emitted fluorescence was measured at 525 nm (525/40 nm BP). The CytExpert software was used to analyse the results.

Samples to determine the abundance of free-living bacteria were preserved using the same method as for phytoplankton. Before analysis, samples were thawed in the dark at room temperature, diluted in a solution of Tris-EDTA buffer (Sigma, C_f = 0.1%) and stained with SYBER-Green I (Molecular Probes Inc, C_f = 0.01%) in a final volume of 5 mL to reach a sufficient amount of bacteria (Marie et al. 1997). Samples were placed in a 80°C

water bath for 15 min in the dark to optimize bacteria staining (Marie et al. 1997). After a 30 min cooling period at room temperature, counts were completed using a BD FACS Calibur Flow Cytometer. The distinction of bacteria was based on groups observed in scatter plots of side scatter (SSC) versus green DNA dye fluorescence signal such as described in Marie et al. (1997), Larsen et al. (2008) and Lapoussière et al. (2011).

To determine the abundance of particle-attached bacteria, seawater subsamples (50 mL) were filtered onto 5 µm Nuclepore polycarbonate membrane. Filters were then placed into cryovials in a 4.95 mL solution of 0.2 µm filtered seawater and 0.05 mL of 50% glutaraldehyde (Grade I, Sigma), gently homogenized and kept in the dark for 15 min at room temperature, and stored at -80°C until analysis by flow cytometry. Prior to analysis, samples were thawed in the dark at room temperature. Membrane filters were rinsed and sonicated for 15 s in 15 mL of a 0.002 M sodium pyrophosphate solution added to water from the cryovials. Subsamples were then diluted, stained and analyzed in the same manner as the treatment for free-living bacteria (Lapoussière et al. 2011).

TEP concentrations were determined using the colorimetric method described in Passow & Alldredge (1995) and Annane et al. (2015). Subsamples (216 ml) were preserved in 24 mL of 20% formaldehyde buffered with hexamethylenetetramine (Parsons et al. 1984) and stored in the dark at 4°C until analysis. Prior to analysis, a subsample (40-45 mL) of the preserved sample was filtered through a 0.4 µm Nuclepore polycarbonate membrane filter at a pressure < 5 mbar. TEP remaining on filters were stained for 5 s with 500 µl of an Alcian Blue solution (0.02% aqueous Alcian Blue in 0.06% glacial acetic acid). Membrane filters were rinsed with 1.5 mL of deionized water and immersed in sulfuric acid (6 mL) for 2 h. TEP in the supernatant were measured with a spectrophotometer at 787 nm. A Xanthan gum calibration was used to transform the values obtained in to Xanthan gum per liter (µg XG eq. L^{-1}).

Subsamples (20 mL) for the identification and enumeration of protists > 3µm were preserved in acidic Lugol's solution (Parsons et al. 1984) and stored in the dark at 4°C. Cell

identification was carried out on two randomly selected mesocosm of the same treatment (duplicate) on day 2, 8 and 14 using an inverted microscope (Wild Heerbrugg) following Lund et al. (1958). The main taxonomic reference used to identify the protist cells was Bérard-Therriault et al. (1999).

To compare biological variables, most values obtained were converted into carbon equivalent. Chl *a*, pheopigments and TEP concentrations were converted into carbon biomass using constant factors of 50 µg C (µg chl *a*)$^{-1}$ (Levasseur et al. 1992), 33 µg C (µg pheopigment)$^{-1}$ (Buck et al. 1995) and 0.75 µg C (µg XG eq. L^{-1})$^{-1}$(Engel & Passow 2001), respectively. Abundances estimated by flow cytometry and microscopy were converted into carbon using conversion factors presented in Table 2.

Table 2. Carbon conversion factors for heterotrophic bacteria, eukaryotic phytoplankton and heterotrophic nanoflagellates

	Carbon conversion factor	**Reference**
Free-living bacteria	14 fg C cell^{-1}	Zubkov et al. 2001
Particle-attached bacteria	50 fg C cell^{-1}	Simon et al. 1990
Picophytoplankton	1500 fg C cell^{-1}	Sherr et al. 2006
Nanophytoplankton	22.5 pg C cell^{-1}	Conversion factor for *Skeletonema costatum* (Harrison et al. 2015)
Heterotrophic nanoflagellates	8.8 pg C cell^{-1}	Holligan et al. 1984

2.3 Sinking velocity experiments

Sinking velocities of chl *a*, pheopigments, bacteria, pico- and nanophytoplankton, heterotrophic nanoflagellates and TEP were measured on two randomly-selected mesocosms for each treatment on every second day from day 0 using settling columns (SETCOL) (Bienfang 1981). The SETCOL consisted of a Plexiglas cylinder of 0.48 min height and a diameter of 0.1 m equipped with ports for subsample removal at the top, middle, and bottom sections of the column.

The mesocosm water subsample was gently mixed before being added to the SETCOL and to a separate 0.5 L control bottle. The SETCOL and the control bottle were kept aside in the dark at a temperature of 8°C for a period of 4 h (± 5 min). After this settling period, the seawater in the bottom section (0.4 L) of the column was collected in a 0.5 L bottle. Samples from both bottles were analyzed as described in Section 2.2.

Sinking velocities (V in m d^{-1}) were calculated according to:

$$V = \frac{B_s}{B_t} \times \frac{h}{t}$$

where B_s is the biomass in the bottom section of the column after the settling period, B_t is the biomass in the control bottle to know the biomass in the homogenous sampled from the mesocosm, h is the height of the column (in m) and t is the settling period (in d) (Riedel et al. 2006). The difference between B_s and B_t in relation with the column dimension gives a measurement of how fast the matter sinks. Potential vertical flux (mg C m^{-2} d^{-1}) were estimated by multiplying carbon concentration by its sinking velocity (Bienfang 1981, Riedel et al. 2006).

2.4 Calculations and statistical analyses

For each mesocosm, variables were integrated over the experiment duration by trapezoidal integration. These values were then divided by the duration of the experiment

(in d) to obtain mean integrated values. The average and standard deviation (SD) or standard error (SE) of replicated measurements are shown in the figures and tables.

Prior to statistical analysis, each variable was tested for homoscedasticity (Levene's test) and normality of distribution (Shapiro-Wilk normality test). When required, a logarithmic or square-root transformation was applied to the data. When normality and homoscedasticity tests failed, a non-parametric test was used. A one-way analysis of variance (ANOVA) or a Kruskall-Wallis test was performed to seek significant difference between treatments. In the event of a significant difference, post-hoc Tukey HSD (Honestly Significant Difference) or Dunn test was carried out for pairwise comparisons.

For the variables with repeated measurements, a linear mixed-effects model was used in order to test the difference between treatments and sampling days with the mesocosms as the random factor (Gałecki & Burzykowski 2013). In the event of a significant difference between treatments, the estimated marginal means was calculated with the Tukey method to identify treatments that were significantly different. When a significant difference was denoted using the linear mixed-effects model, results of the post-hoc tests were represented in letters above the mean integrated values ($a > b > c > d$). All statistical analyses were performed using the R software (version 3.6.3).

3 RESULTS

3.1 Nutrients

NO_3, PO_4 and $Si(OH)_4$concentrations decreased by $\sim 20\%$ between nutrient enrichment of the mesocosms on day -1 and the onset of the experiment on day 0 (Table 1, Fig. 1). Nutrient concentrations further decreased in all mesocosms starting on day 0; mesocosms were depleted in NO_3 after day 1, in $Si(OH)_4$ after day 2, and in PO_4 after day 5

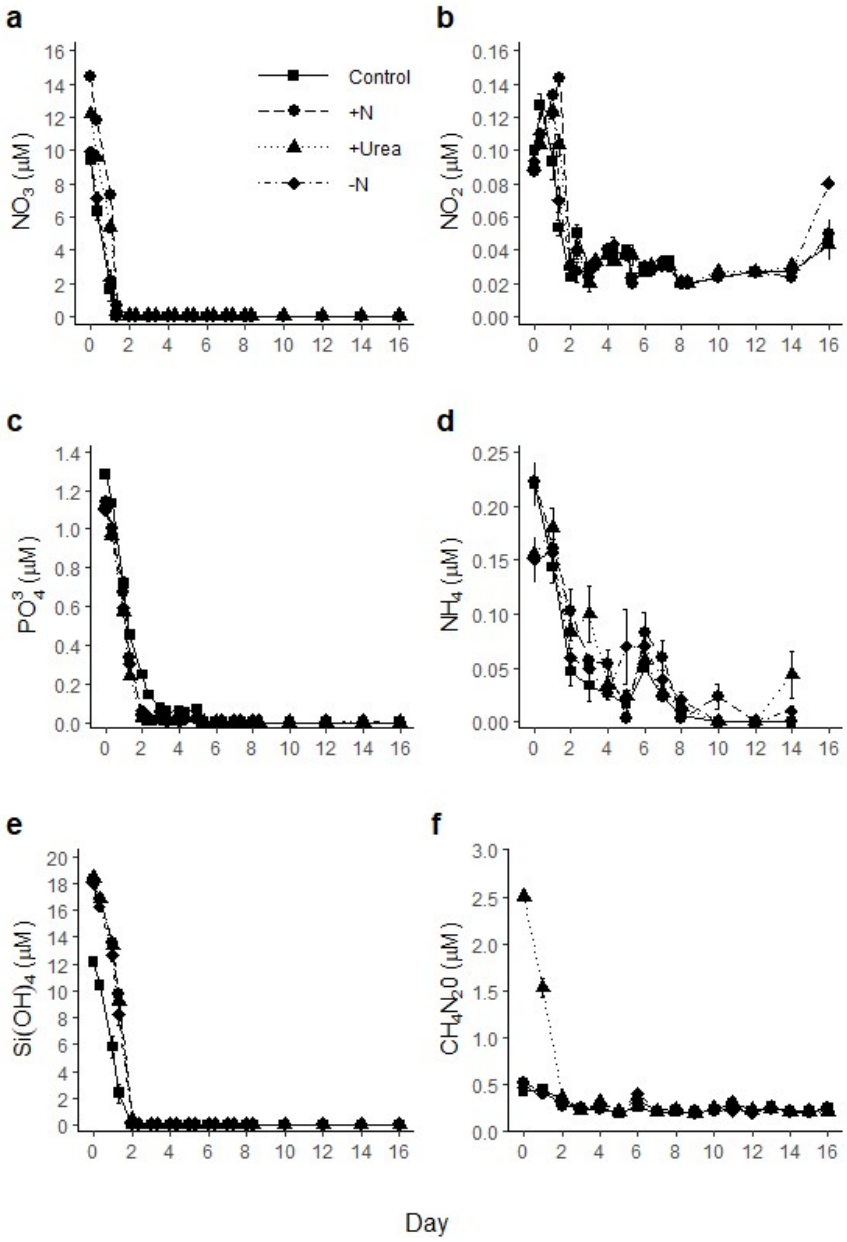

Figure 1. Temporal variations of daily-averaged concentrations of a) nitrate, b) nitrite, c) phosphate, d) ammonium, e) silicic acid and f) N-urea for the control, +N, +Urea and –N treatments. The error bars represent the standard error of three replicated measurements. Note the different vertical scales

(Fig. 1). NO_2 concentrations first increased from ~ 0.09 to 0.14 µM then decreased, fluctuated and then increased gradually to ~ 0.05 µM at the end of the experiment. Ammonium concentration decreased from ~ 0.2 µM to ~ 0.05 µM on day 5 and fluctuated from < 0.02 µM to 0.08 µM during the rest of the experiment. Urea concentration decreased from 2.5 µM on day 0 to ~ 0.4 µM on day 2 in the +Urea treatment and from ~ 0.5 µM on day 0 to ~ 0.35 µM on day 3 in the other treatments. N-urea remained relatively constant around 0.3 µM afterward.

Nutrient consumption rates between day 0 and day 2 are presented in Table 3. NO_3 consumption rates were higher in the +N and +Urea treatments than in control and –N treatments. During this period, NO_3 was the main form of dissolved nitrogen consumed by the planktonic community of this experiment, accounting for > 90% in control, +N and –N treatments and 73% in the +Urea treatment (Table 3). The PO_4 and $Si(OH)_4$ consumption rates were similar in all treatments. The ratio of NO_3:PO_4 consumption was significantly higher in the nitrogen enriched treatments while NO_3:$Si(OH)_4$ consumption ratio was significantly lower the +Urea and –N treatments compared to the control (Table 4). The atomic ratio of total dissolved nitrogen to silicic acid was significantly lower in the –N treatment in comparison. However, no significant difference was found between treatment for the ratio of silicic acid and biogenic silica nor for the diatom-specific consumption rate of $Si(OH)_4$ (Table 4).

A relative preference index (RPI) was calculated to compare how one form of nitrogen is preferably selected relatively to another nitrogen form also present in the ambient environment (McCarthy et al. 1977; Table 5). As the concentrations of nitrogenous nutrients decreased during the first two days, we assumed that nitrogen regeneration rates were low compared to their consumption rates. An RPI of 1 indicates that a form is used in proportion to its availability. NO_3 was the preferred form of nitrogen used in all treatments (RPI > 1; Table 5). It was followed by NO_2, NH_4 and N-urea (RPI ranging from 0.877 to

0.222), except in the +Urea treatment where N-urea was preferred over NO_2 and NH_4 (RPI = 0.899; Table 5).

Table 3. Nutrient consumption rates in each mesocosms treatment from day 0 to day 2. The percent contribution of each nitrogenous nutrient to total nitrogen consumption is also represented. Mean values ± SD are shown. Values in bold significantly differ from Control (see Table S1)

	Control	**+N**	**+Urea**	**–N**
ρNO_3 ($\mu M\ d^{-1}$)	4.72 ± 0.372	**7.22 ± 0.070**	**6.09 ± 0.112**	4.94 ± 0.420
% at.N	96	96	73	96
ρNO_2 ($\mu M\ d^{-1}$)	0.04 ± 0.008	0.03 ± 0.003	0.03 ± 0.001	0.03 ± 0.006
% at.N	0.78	0.38	0.36	0.61
ρNH_4 ($\mu M\ d^{-1}$)	0.09 ± 0.012	0.06 ± 0.030	0.04 ± 0.015	0.04 ± 0.025
% at.N	1.76	0.79	0.48	0.87
ρN-urea ($\mu M\ d^{-1}$)	0.04 ± 0.008	0.12 ± 0.015	**1.07 ± 0.051**	0.07 ± 0.037
% at.N	1.8	3.3	26	2.6
ρPO_4 ($\mu M\ d^{-1}$)	0.52 ± 0.014	0.55 ± 0.016	0.55 ± 0.003	0.52 ± 0.020
$\rho Si(OH)_4$ ($\mu M\ d^{-1}$)	6.05 ± 0.254	9.10 ± 0.097	8.96 ± 0.505	8.85 ± 0.323

Table 4. Nutrient consumption ratios between day 0 and day 2, dissolved silicon consumption rate over biogenic silica accumulation rate between day 0 and day 2 and over diatom abundance on day 2. Mean values± SD are presented. Values in bold significantly differ from Control (see Table S2)

	Control	**+N**	**+Urea**	**–N**
ρNO_3:ρPO_4 (d:d)	9.13 ± 0.279	**13.09 ± 0.241**	**11.10 ± 0.098**	9.54 ± 0.377
ρNO_3:$\rho Si(OH)_4$ (d:d)	0.78 ± 0.014	0.79 ± 0.007	**0.68 ± 0.019**	**0.56 ± 0.020**
ρTDN: ρSi (d:d)	0.81 ± 0.014	0.83 ± 0.010	**0.93 ± 0.030**	**0.58 ± 0.020**
$\rho Si(OH)_4$/ρBSi (d:d)	1.74 ± 0.308	2.62 ± 0.304	1.85 ± 0.306	1.85 ± 0.088
$\rho Si(OH)_4$/diatom (pmol Si diatom^{-1} d^{-1})	0.16 ± 0.018	0.19 ± 0.012	0.17 ± 0.013	0.21 ± 0.033

Table 5. Relative preference index (RPI) of the microbial community for different nitrogenous nutrients in each mesocosm treatment from day 0 to day 2. Higher RPI indicates higher preference (McCarthy et al. 1997). Mean values± SD are shown. There was no significant differences between treatments (see Table S3)

	Control	**+N**	**+Urea**	**–N**
Nitrate	1.074 ± 0.006	1.045 ± 0.007	1.050 ± 0.016	1.073 ± 0.020
Nitrite	0.823 ± 0.027	0.682 ± 0.026	0.700 ± 0.011	0.724 ± 0.035
Ammonium	0.877 ± 0.147	0.568 ± 0.312	0.487 ± 0.197	0.625 ± 0.141
N-urea	0.222 ± 0.023	0.498 ± 0.038	0.899 ± 0.033	0.313 ± 0.165

3.2 Pigments and particulate matter

For all the concentrations, the time had a significant impact meaning that a bloom was successfully induced in the mesocosms. Chl *a* concentrations rapidly increased from day 0 to day 2 and gradually decreased until the end of the experiment for all treatments (Fig. 2). Throughout the experiment, chl *a* concentrations were significantly higher in the two nitrogen-enriched treatments than in control and –N. The percent increase in +N and +Urea treatments relative to the control was 62% and56%, respectively (Fig. 2, Table 6). In contrast to chl *a*, pheopigment concentrations increased from day 0 to day 6 and decreased moderately from day 10 onward. Pheopigments were significantly lower in the –N treatment (-28%) compared to the control. Total pigments (i.e., the sum of chl *a* and pheopigments) were higher in the +N (46%) and +Urea (44%) treatments compared to the control, whereas there was no significant difference between the –N treatment and control.

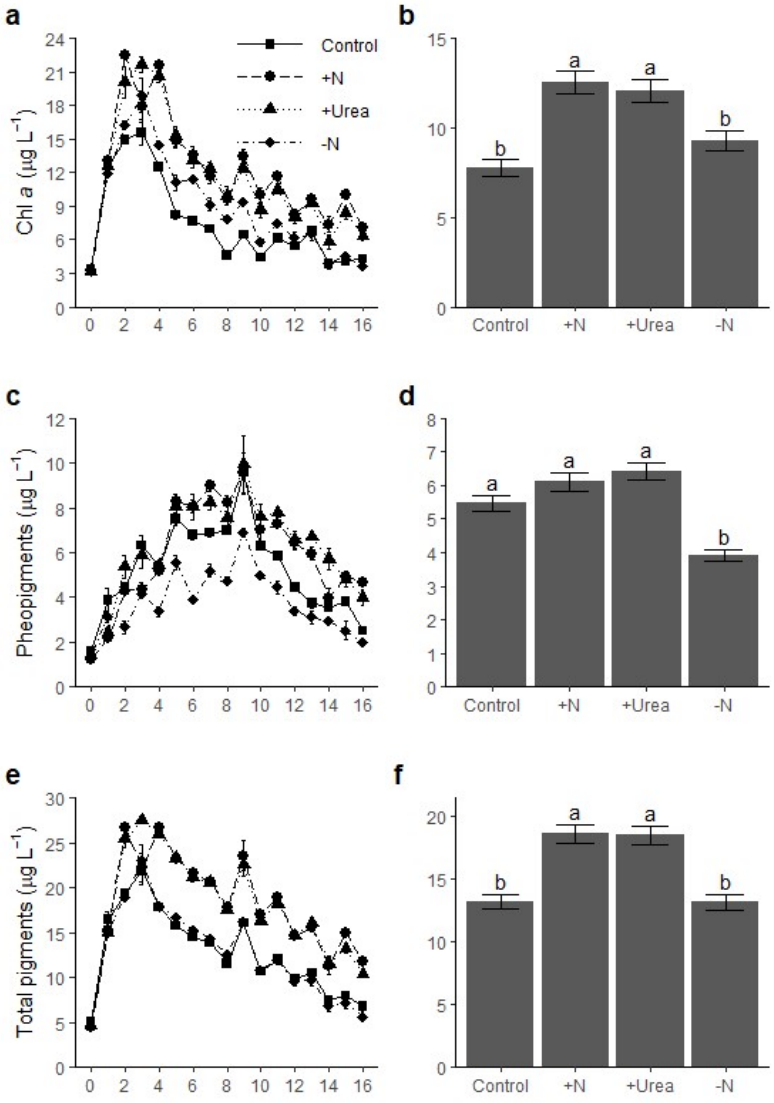

Figure 2. Temporal variations and integrated means over time of the concentration of a-b) chlorophyll *a*, c-d) pheopigments and e-f) total pigments (i.e., the sum of chlorophyll *a* and pheopigments) for the control, +N, +Urea and –N treatments. The error bars represent the standard error of three replicated measurements. There is a significant difference between treatments ($p < 0.05$). The pairwise comparison post-hoc test denotes two groups for each variable where a > b. Note the different vertical scales

Table 6. Percentage increase or decrease from the mean control for different biological variables studied. Values in bold are significantly different from those in control ($p < 0.05$)

Concentrations	Control mean value	% +N	% +Urea	% –N
Chl *a* (μg C L^{-1})	387.29	**62**	**56**	20
Pheopigments (μg C L^{-1})	180.33	12	17	**-28**
Total pigments (μg C L^{-1})	567.62	**46**	**44**	4
PON (μM)	14.33	**24**	**25**	-1
POP (μM)	0.91	10	12	1
BSi (μM)	12.41	13	17	16
Picophytoplankton (μg C L^{-1})	41.33	-6	-17	-14
Nanophytoplankton (μg C L^{-1})	456.66	**29**	**33**	24
Heterotrophic flagellates (μg C L^{-1})	151.18	34	38	10
Free-living bacteria (μg C L^{-1})	0.39	5	7	0
Particle attached bacteria (μg C L^{-1})	0.33	11	22	-1
TEP (μg C L^{-1})	629.17	20	14	7
Total biogenic carbon (μg C L^{-1})	1442.55	**24**	**22**	8
Sinking velocities (m d^{-1})				
Chlorophyll *a*	0.20	0	0	42
Pheopigments	0.30	-7	-5	46
Total pigments	0.24	0	-8	47
Picophytoplankton	0.06	40	28	0
Nanophytoplankton	0.16	3	-5	75
Heterotrophic nanoflagellates	0.13	-26	-42	-9
Free-living bacteria	0.05	-83	-28	-68

Particle attached bacteria	0.24	-15	-47	-5
TEP	0.15	-18	-4	37
Downward fluxes (mg C m^{-2} d^{-1})				
Chlorophyll *a*	69.93	107	70	62
Pheopigments	36.23	7	8	1
Total pigments	106.16	73	68	41
Picoeukaryotes	1.49	52	7	-18
Nanoeukaryotes	85.25	22	23	101
Heterotrophic nanoflagellates	14.04	-15	-9	60
Free-living bacteria	0.01	-69	2	-86
Particle attached bacteria	0.06	18	-28	7
TEP	94.91	-5	9	55
Total biogenic carbon	270.07	4	-6	45

During the first day of the experiment, the ratio of pheopigments to total pigments decreased from ~ 30% to 22% in the control and to ~ 14% in the other treatments. It gradually increased up to 60% in the control and ~ 45% in the other treatments on days 8-10 and then decreased to ~ 40% at the end of the experiment (Fig. S1). The overall mean ratio was significantly higher in the control than in the other treatments.

PON, POP and BSi concentrations showed a large increase in all treatments at the beginning of the experiment, followed by a gradual decrease (Fig. 3). PON concentrations were higher in the nitrogen-enriched treatments than in the control and –N, whereas POP and BSi concentrations were not significantly affected by the treatments (Table 6).

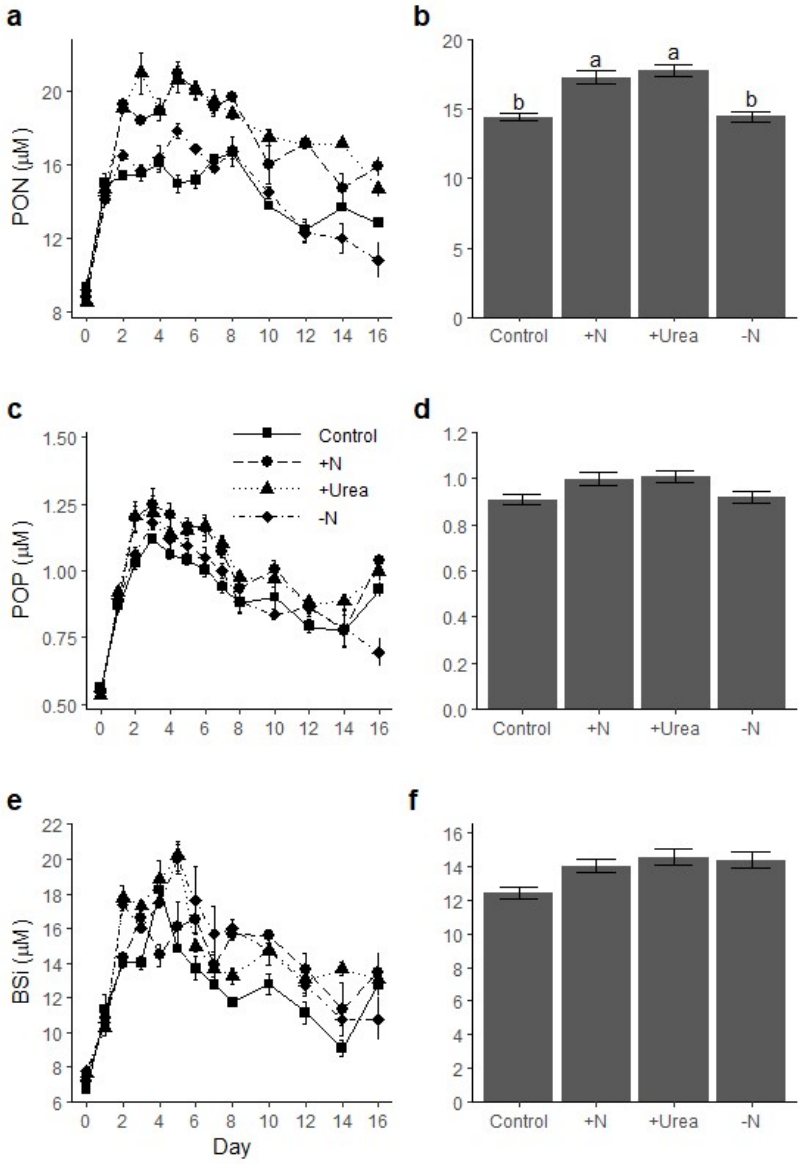

Figure 3. Temporal variations and integrated means of the concentrations of a-b) particulate organic nitrogen (PON), c-d) particulate organic phosphorus (POP) and e-f) biogenic silica (BSi) for the control, +N, +Urea and –N treatments. The error bars represent the standard error of three replicated measurements. There is a significant difference between treatments for PON ($p < 0.05$). The pairwise comparison post-hoc test denotes two groups where a > b. Note the different vertical scales

3.3 Phytoplankton, heteroflagellates, bacteria and TEP

The carbon biomass of picophytoplankton, nanophytoplankton and heterotrophic nanoflagellates displayed different temporal trends during the experiment (Fig. 4). Picoeukaryotes increased during the first two days followed by a gradual decrease to reach low biomass on day 16 in all treatments. The +Urea and –N treatments had a phytoplankton carbon biomass in average ~ 15% lower than the control throughout the experiment and there was no significant difference between +N treatment and control (Table 6). The temporal variation in nanophytoplankton carbon biomass followed a bell shape with maximum carbon biomass on day 6 in all treatments, with significantly higher carbon biomass in the nitrogen-enriched treatments than in the control (~ 30%). The carbon biomass of heterotrophic flagellates was not different between treatments. The pattern over time was inversely similar to picophytoplankton biomass with minimum values between day 0 and 6, and a gradual increase afterwards until a maximum around day 14.

The temporal variation in free-living bacteria carbon biomass was similar in all treatments to that of picophytoplankton, except for a decline starting around day 4 instead of day 2 (Figs. 4a and 5a). The particle-attached bacteria carbon displayed a small decline from day 4 to day 8 followed by a gradual recovery until the end of the experiment (Fig. 5c). There was no significant difference between the treatments and the control for both free-living and particles-attached bacteria carbon. TEP carbon concentrations increased from day 0 to day 4, stayed relatively constant up to day 12, and then increased until the end of the experiment. The carbon biomass of particle-attached bacteria was positively correlated to TEP concentrations in control, +N and –N treatments ($p \leq 0.001$), and in the +Urea treatment ($p < 0.01$) (Fig. S2).

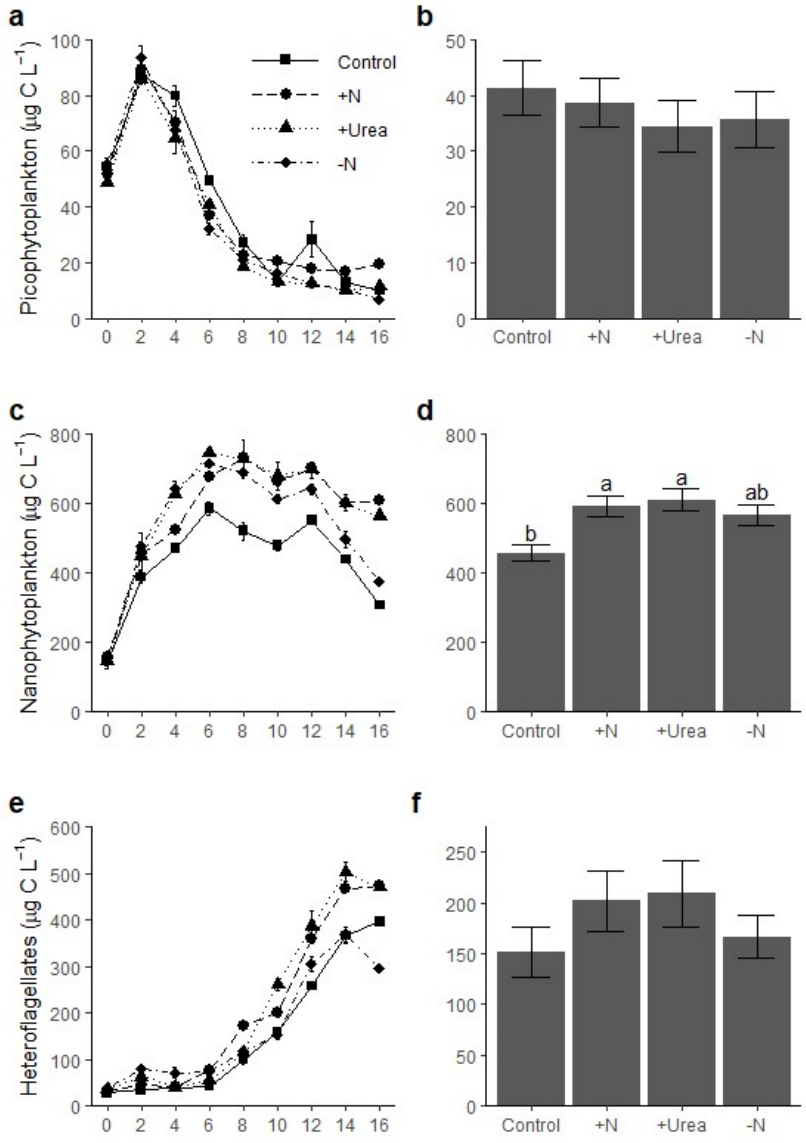

Figure 4. Temporal variations and integrated means of the carbon biomass of a-b) picophytoplankton, c-d) nanophytoplankton, and e-f) heterotrophic nanoflagellates for the control, +N, +Urea and –N treatments. The error bars represent the standard error of two replicated measurements. There is a significant difference between treatments for nanoflagellates ($p < 0.05$). The pairwise comparison post-hoc test denotes two groups where a > b. Note the different vertical scales

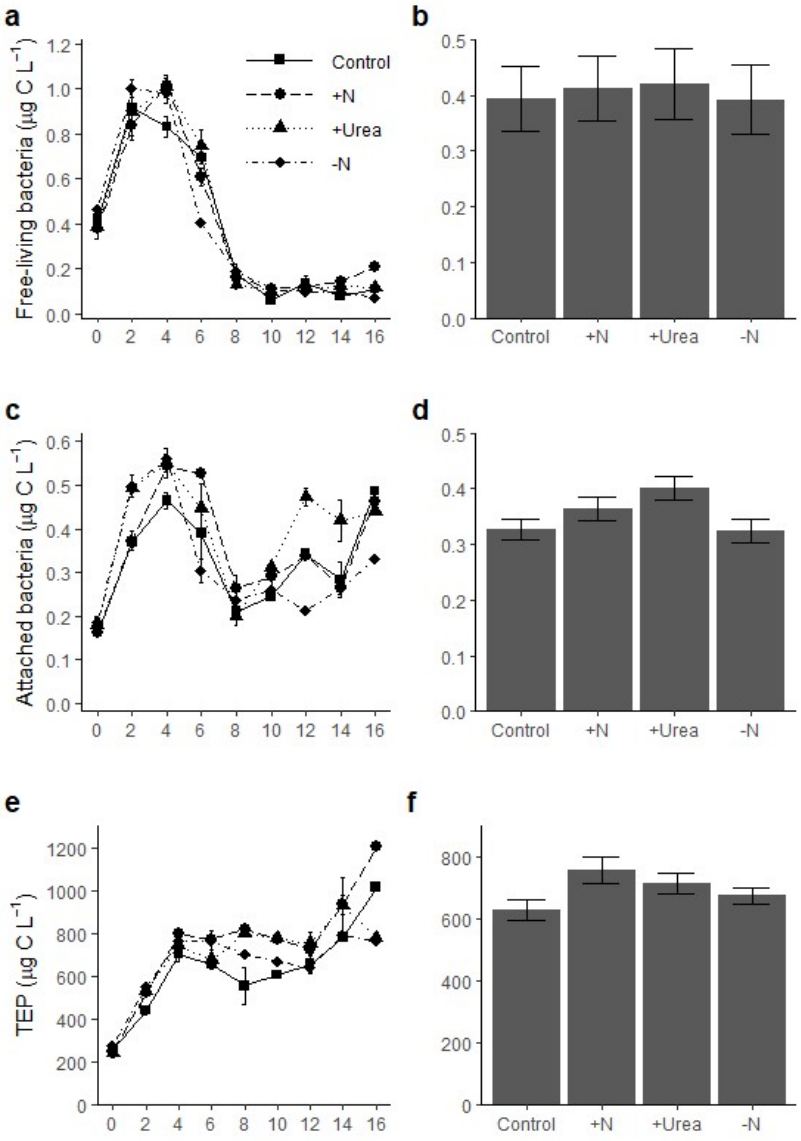

Figure 5. Temporal variations and integrated means of the carbon biomass of a-b) free-living heterotrophic bacteria, c-d) particle-attached heterotrophic bacteria and e-f) transparent exopolymeric particles (TEP) for the control, +N, +Urea and –N treatments. The error bars represent the standard error of two replicated measurements. There was no significant differences between treatments. Note that values are represented on different vertical scales

3.4 Total carbon estimation and relative contributions

The total biogenic carbon in each treatment was estimated as the sum of all microbial components (i.e., picophytoplankton + nanophytoplankton + heterotrophic nanoflagellates + free-living and particle-attached bacteria), TEP, and pheopigments (Fig. 6). The total biogenic concentration was significantly different between each treatment with +N and +Urea in group a, and –N and control in group b. The percent difference relative to the control being 24, 22 and 8%, respectively (Table 6). In terms of contributions, TEP made up about 50% of the total biogenic carbon in all treatments throughout the experiment (Fig. 6c). Nanophytoplankton also represented an important part, followed by heterotrophic nanoflagellates, pheopigments, and then picophytoplankton. Bacteria, both free-living and particle-attached, represented a negligible proportion of the total biogenic carbon.

3.5 Taxonomic composition of protists

Protists ≥ 4 μm were counted in each treatment on days 2, 8 and 14 (Fig. 7). The total cell abundance seemed higher on day 2 than on day 14 in all treatments. The protist community in all treatments was numerically dominated by the chain-forming centric diatom *Skeletonema costatum* (cell size of 4-16 μm) representing up to 75% of the total cell abundances on day 2. However, their absolute and relative abundance generally decreased from day 2 to day 14 in all treatments. The second most dominant genus was *Chaetoceros* spp. (cell size of 4-30 μm), another chain-forming centric diatom. Pennate diatom abundance was always low, contributing < 2% of the total cell abundance. During the experiment, the relative abundance of centric diatoms decreased from ~ 95% on day 2 to ~ 75% on day 14, whereas heterotrophic flagellate abundance increased from ~ 4% to ~ 25% during the same period. The heterotrophic flagellate group was mainly composed of small cells (< 5 μm).

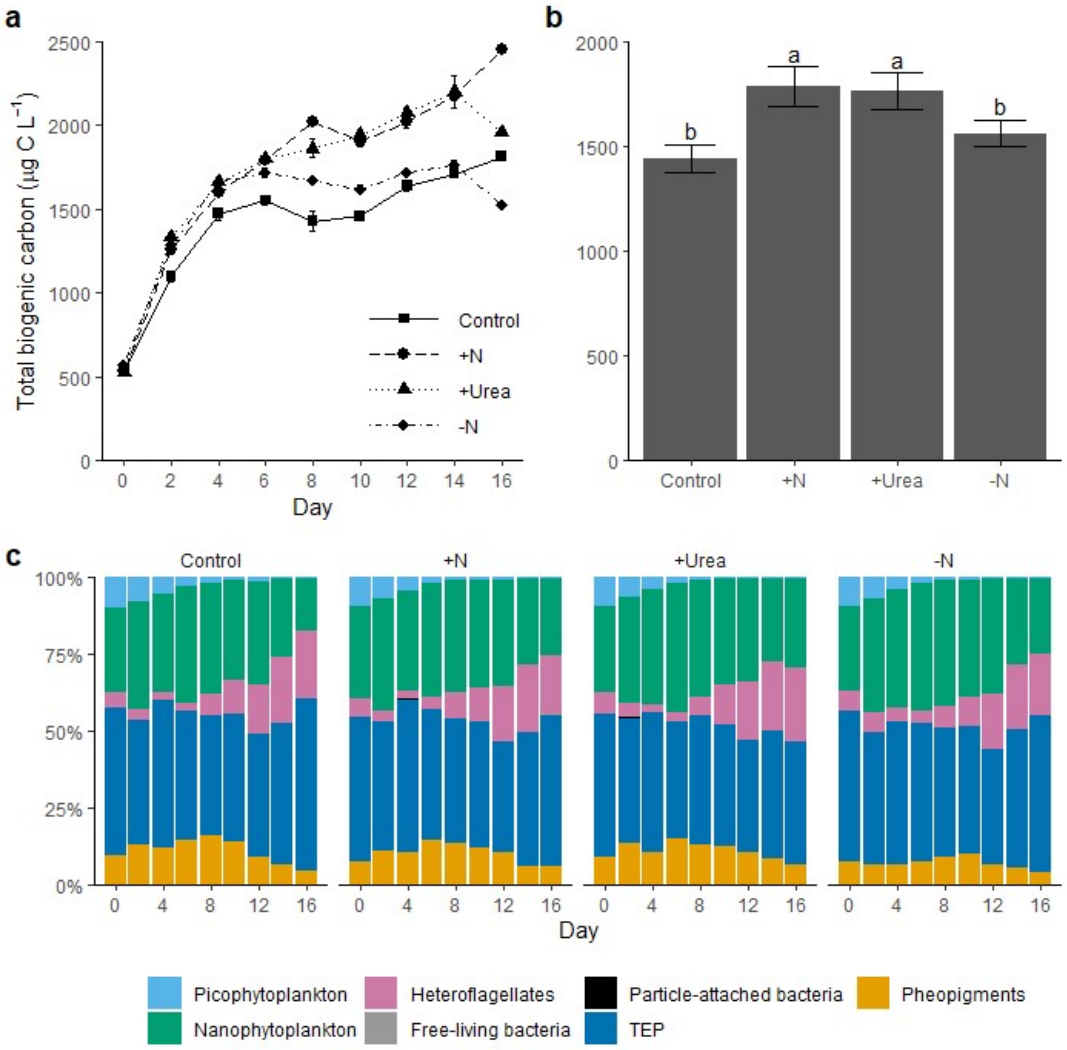

Figure 6. Temporal variations and integrated means of a-b) estimated total biogenic carbon concentrations and c) relative contribution of picophytoplankton, nanophytoplankton, heterotrophic nanoflagellates, free-living and particles-attached bacteria, TEP and pheopigments for the control, +N, +Urea and –N treatments. The relative contribution of free-living and particle-attached bacteria is < 0.5%. There is a significant difference between treatments for the total carbon biomass ($p < 0.05$). The pairwise comparison post-hoc test denotes two groups where a > b.

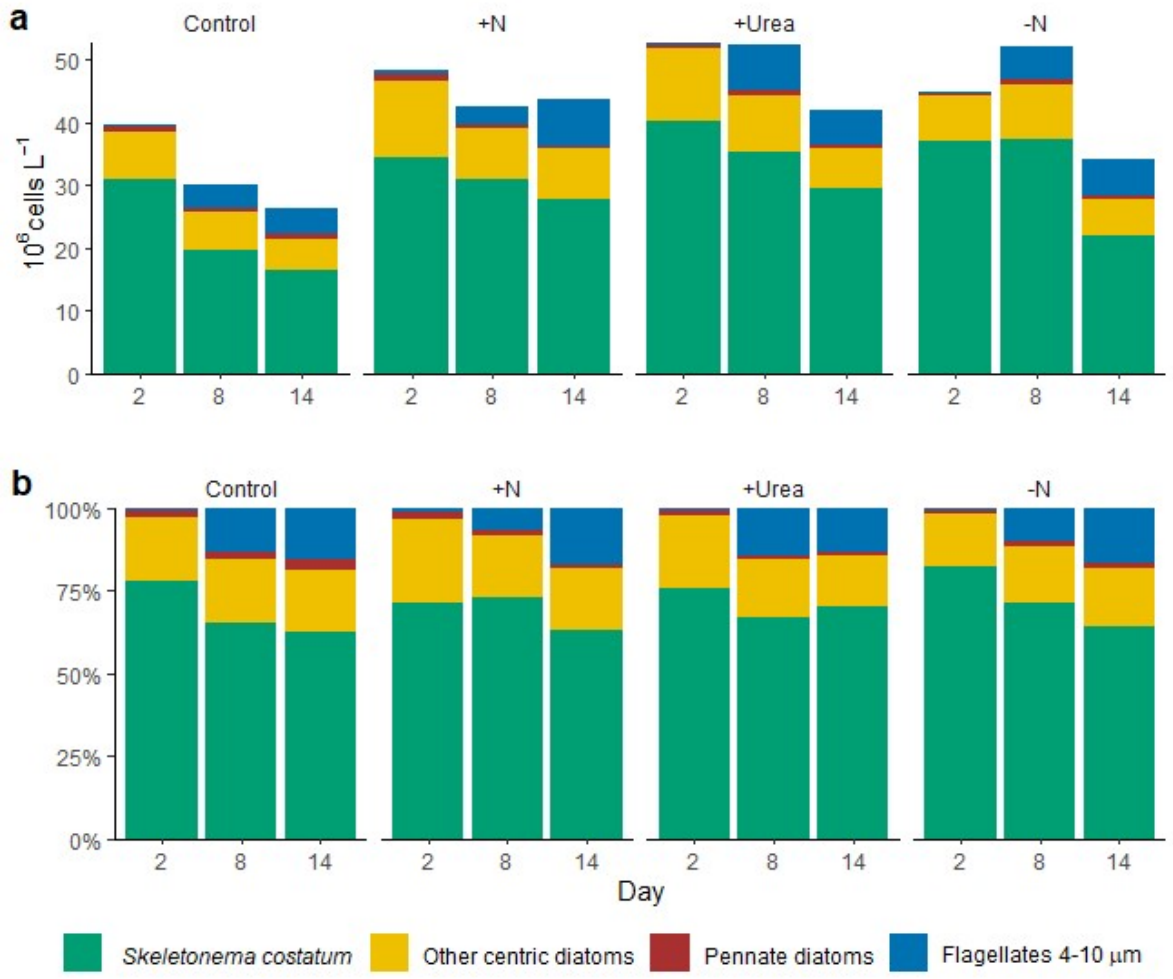

Figure 7. Variations of the a) absolute and b) relative abundance of different taxonomic groups of protists under four experimental treatments on days 2, 8 and 14 for the control, +N, +Urea and –N treatments

3.6 Sinking velocities

The sinking velocity of pigments followed a bell-shaped pattern, increasing from day 0 to day 8 and decreasing during the rest of the experiment for all treatments (Fig. 8). No significant differences in pigments velocities were observed ($p > 0.05$) among treatments. Pigment sinking velocities in the –N treatment showed a large temporal variability compared to the control. Maximum sinking velocities were observed in the –N treatment starting on day 10 for chl *a*, from day 4 to 14 for pheopigments and from day 6 until the end of the experiment for total pigments. Mean sinking velocities of pigments were around 47% higher in the –N treatment than the other treatments (Table 6).

Picophytoplankton had low sinking velocities compared to the other measured variables (Fig. 9). Sinking velocities remained < 0.25 m d^{-1} with a control mean value of 0.06 m d^{-1} (Table 6). Similar to pigment sinking velocities, the maximum sinking velocities for pico- and nanophytoplankton were observed close to day 8. For nanophytoplankton, although there was no significant difference between treatments according to the statistical analysis, the mean sinking values of the –N treatment was high compared to the other treatments (Fig. 10). Sinking velocities of heterotrophic nanoflagellates were ~ 0.15 m d^{-1} on average with inconsistent patterns among treatments.

Sinking velocities of free-living and particle-attached bacteria differed, with free-living bacteria sinking slower than particle-attached bacteria (Figs. 9 and 10). In the second half of the experiment, particle-attached bacteria sank at variable speeds depending on the treatment, with values near zero for the +Urea treatment and reaching maximum values for –N treatment. Maximal TEP sinking velocities were observed on day 8 and were not significantly different among treatments (Fig. 9f).

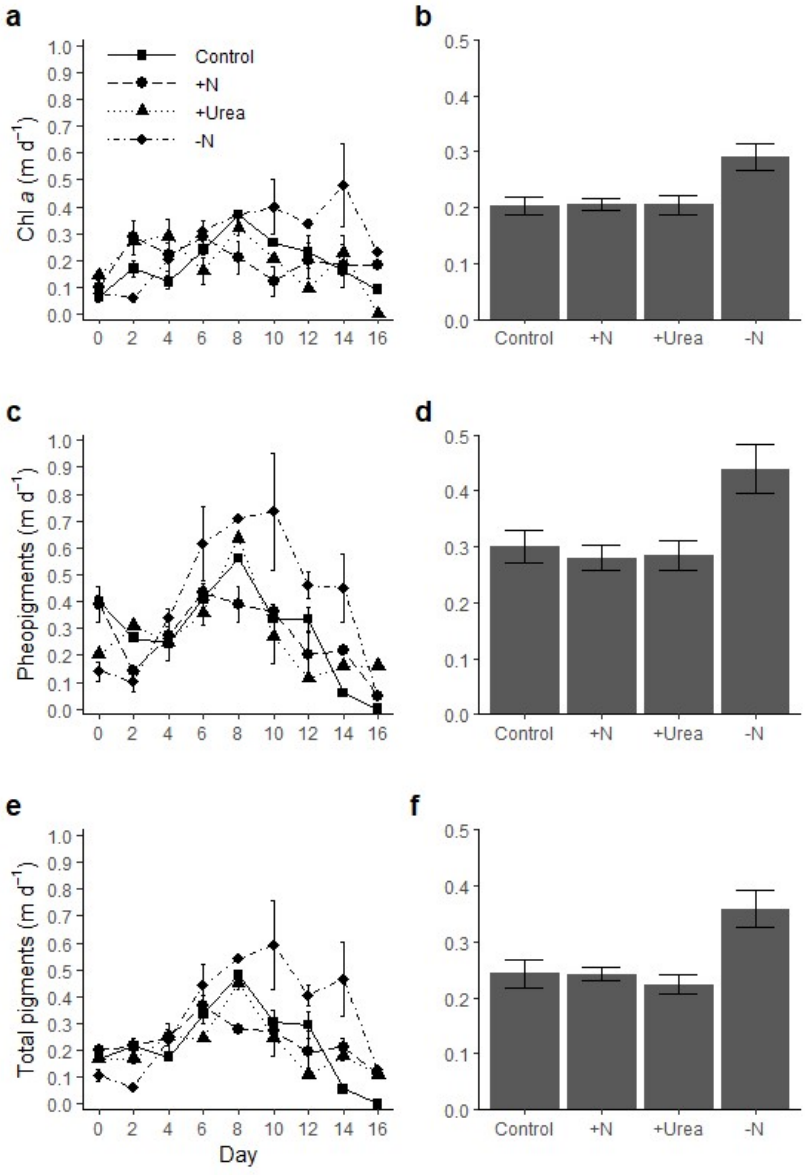

Figure 8. Temporal variations and integrated means of averaged sinking velocities of a-b) chl *a*, c-d) pheopigments and e-f) total pigments for the control, +N, +Urea and –N treatments. The error bars represent the standard error of 2 replicated measurements. There are no significant differences between treatments ($p > 0.05$)

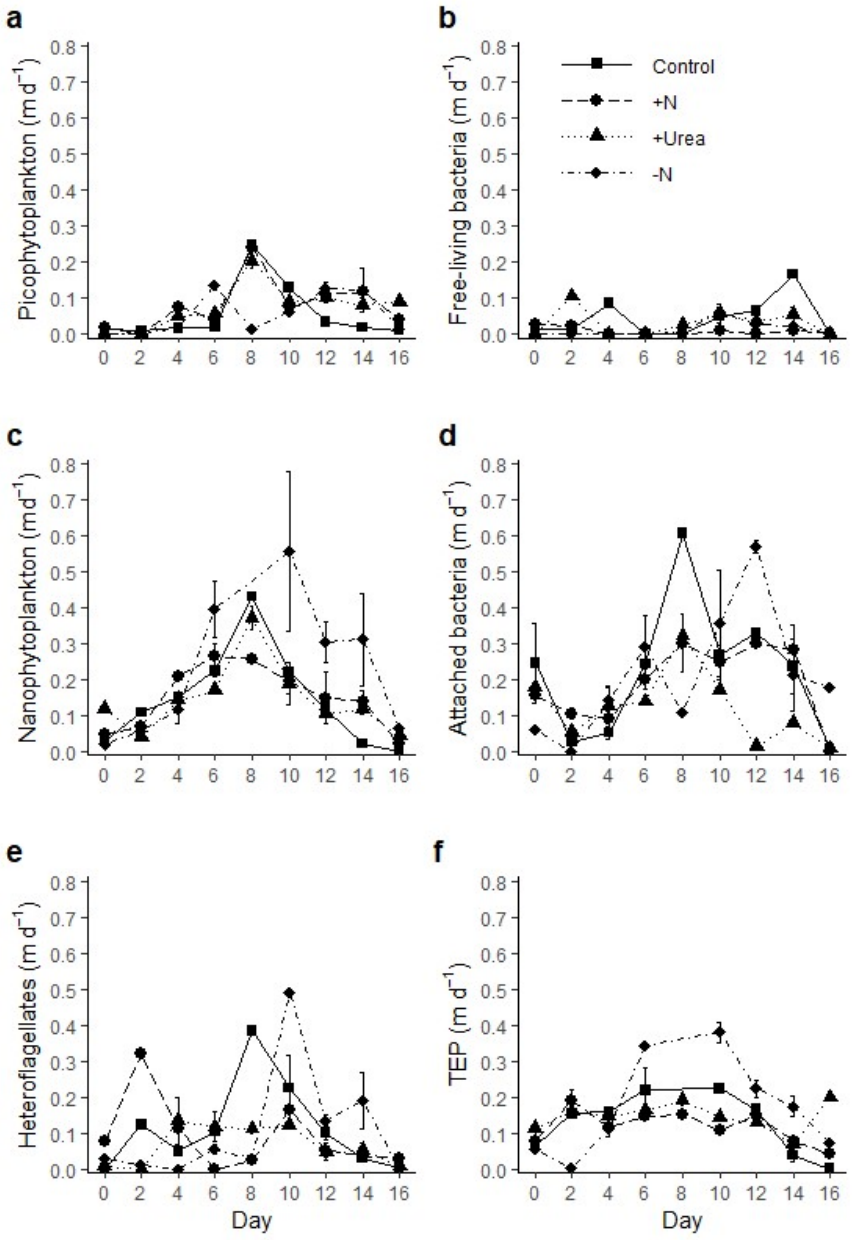

Figure 9. Temporal variations of averaged sinking velocities of a) picophytoplankton, c) nanophytoplankton, e) heterotrophic nanoflagellates, b) free-living and d) particle-attached bacteria, and f) TEP for the control, +N, +Urea and –N treatments. The error bars represent the standard error of 2 replicated measurements

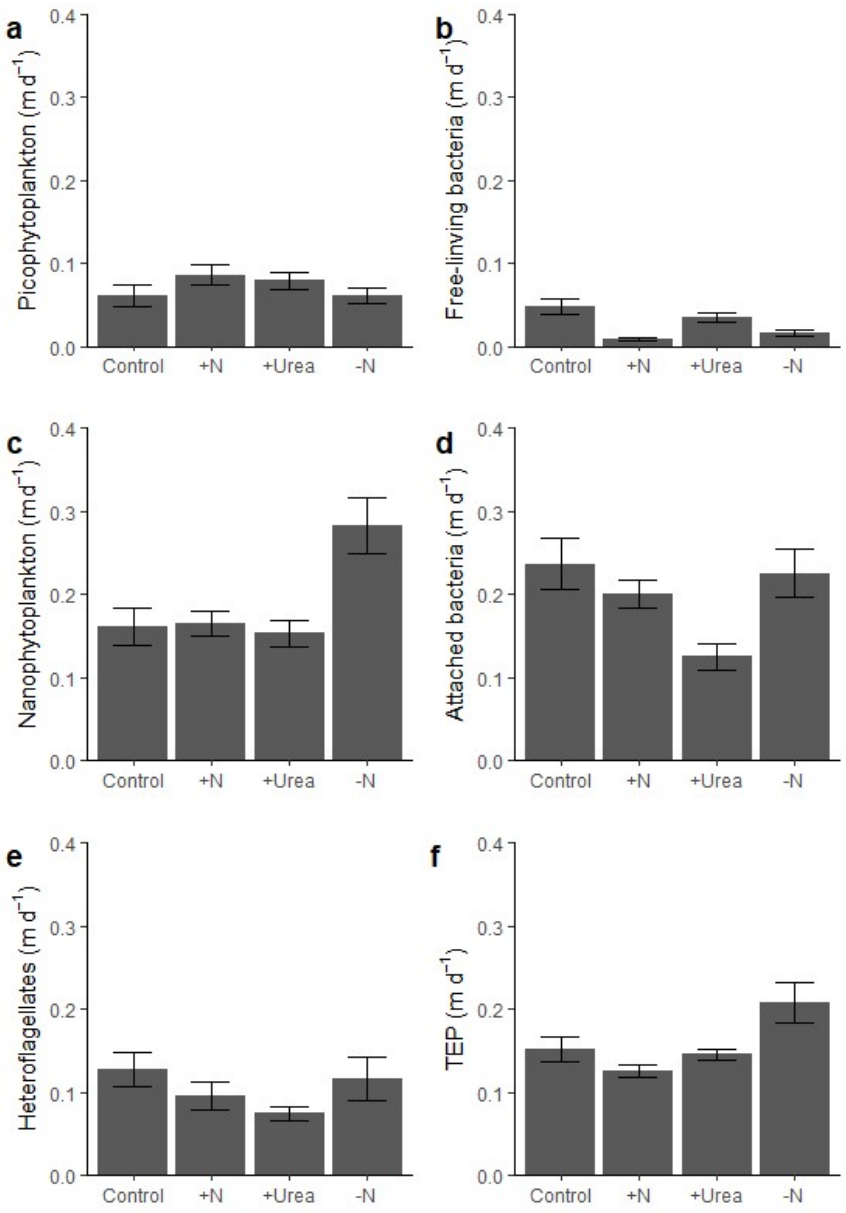

Figure 10. Integrated mean sinking velocities of a) picophytoplankton, c) nanophytoplankton, e) heterotrophic nanoflagellates, b) free-living bacteria, d) particle-attached bacteria and f) TEP for the control, +N, +Urea and –N treatments. The error bars represent the standard error of 2 replicated measurements. There was no significant difference between treatments ($p > 0.05$)

3.7 Downward fluxes

The potential downward fluxes of each parameter were estimated considering their respective carbon concentration and sinking velocity. Chl *a* and total pigment downward fluxes in each treatment showed a large temporal variability during the experiment with values ranging from 0 to 350 mg C m^{-2} d^{-1} (Fig. 11). Pheopigments showed less variability over time with fluxes ranging from 0 to 150 mg C m^{-2} d^{-1}. For pheopigments and total pigments, maximum fluxes were reached between day 6 and day 10 for each treatment. The downward fluxes of chl *a* and total pigments were not significantly different among all treatments. However, the downward fluxes in the nutrient-enriched treatments were in average 62 to 107% higher than in the control for the chl *a* (Table 6).

The downward fluxes of picophytoplankton remained low in all treatments, with a mean of 1.49 mg C m^{-2} d^{-1} and a range from 0 to ~ 6 mg C m^{-2} d^{-1} (Fig. 12). The picophytoplankton carbon flux in the +N treatment was in average 101% higher than in the control. Nanophytoplankton contributed to a major fraction in the carbon downward fluxes. Heterotrophic nanoflagellates sinking fluxes averaged ~ 10 mg C m^{-2} d^{-1} from day 0 to day 6, and 50 mg C m^{-2} d^{-1} later on.

The downward flux of total biogenic carbon followed a bell shape, with a maximum rate around day 10 (Fig. 13). There was no significant difference between treatments although the maximum carbon fluxes occurred in the –N treatment from day 6 to day 14. During the experiment, the fluxes in the control, +N and +Urea treatments varied between 1.5 and 700 mg C m^{-2} d^{-1}, with a mean value of 270 mg C m^{-2} $d^{-1}$for the control (Table 6). In the –N treatment, the fluxes ranged from 20 to 725 mg C m^{-2} d^{-1}, with a mean value of 363 mg C m^{-2} d^{-1}.

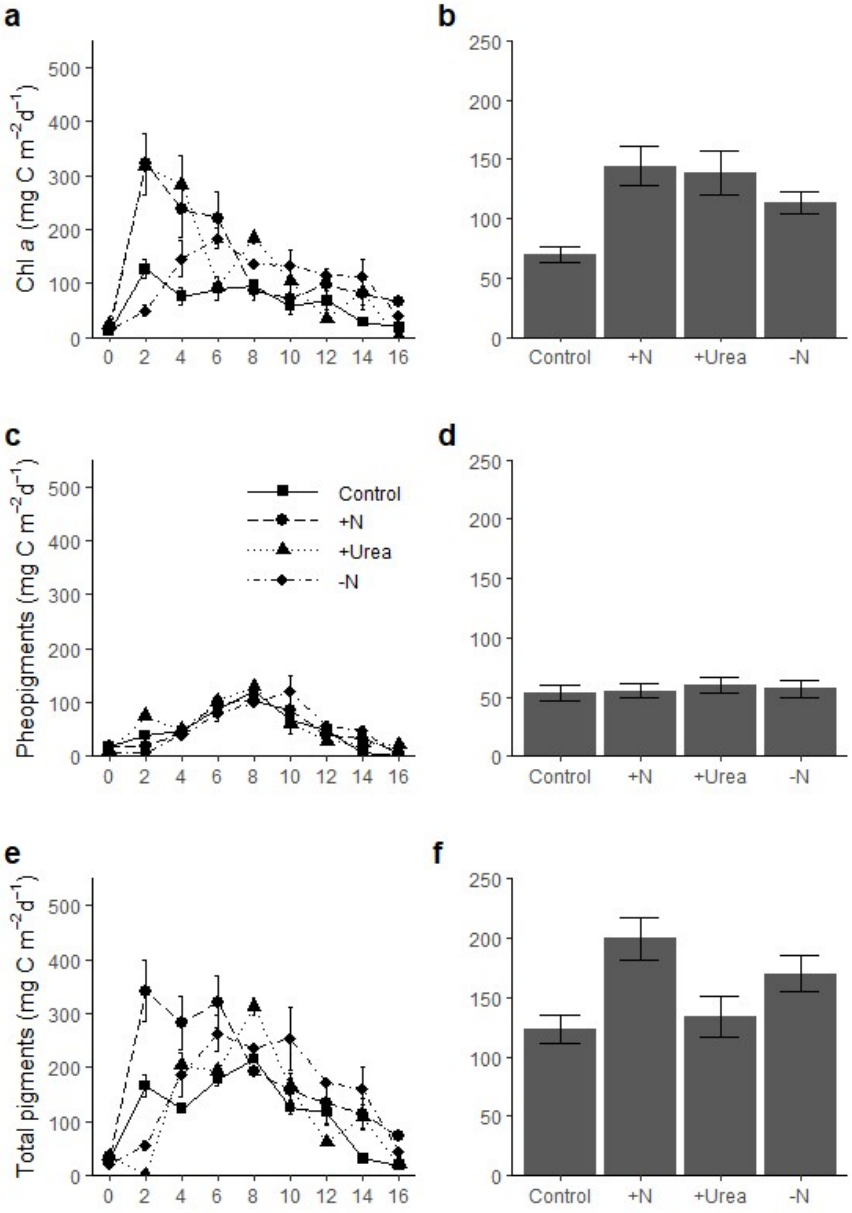

Figure 11.Temporal variations and integrated means of averaged downward fluxes of a-b) chlorophyll *a*, c-d) pheopigments and e-f) total pigments for the control, +N, +Urea and –N treatments. The error bars represent the standard error of 2 replicated measurements. There was no significant difference between treatments ($p > 0.05$)

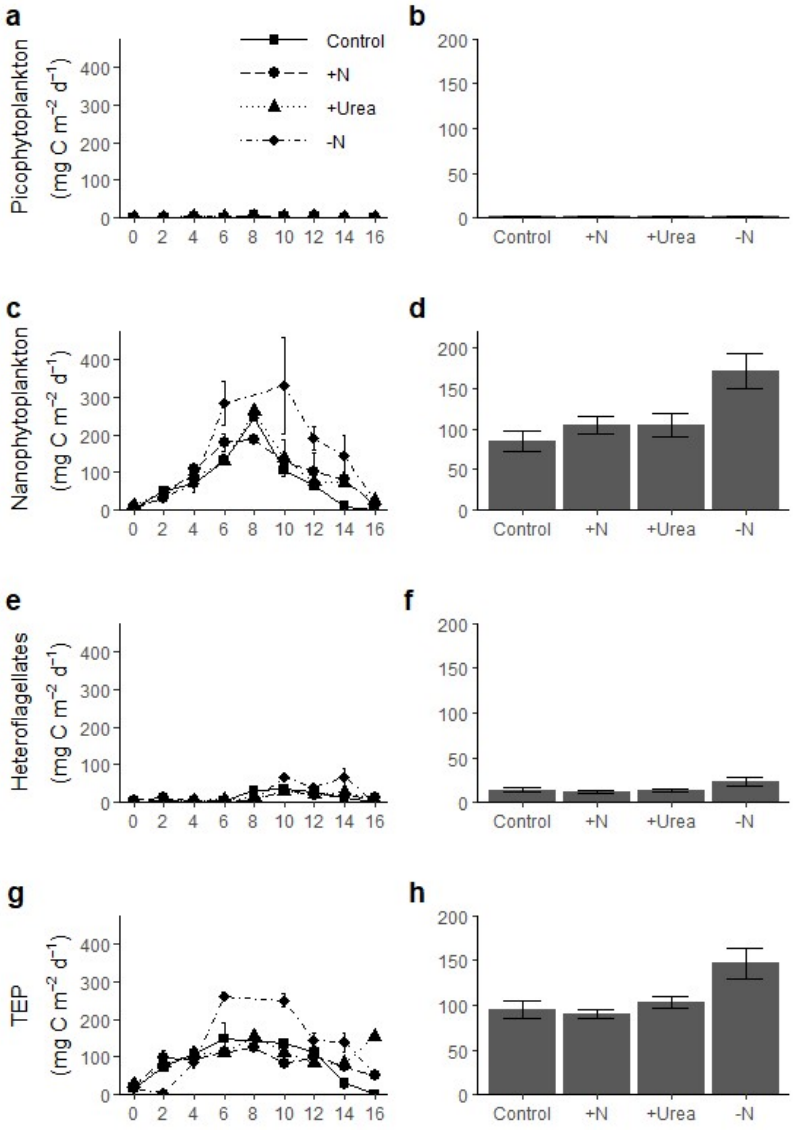

Figure 12. Temporal variations and mean integrated values of averaged downward fluxes of a-b) picophytoplankton, c-d) nanophytoplankton, e-f) heterotrophic nanoflagellates and g-h) TEP for the control, +N, +Urea and –N treatments. Picophytoplankton fluxes are lower than 6 mg C m^{-2} d^{-1}. The error bars represent the standard error of 2 replicated measurements. There was no significant difference between treatments ($p > 0.05$)

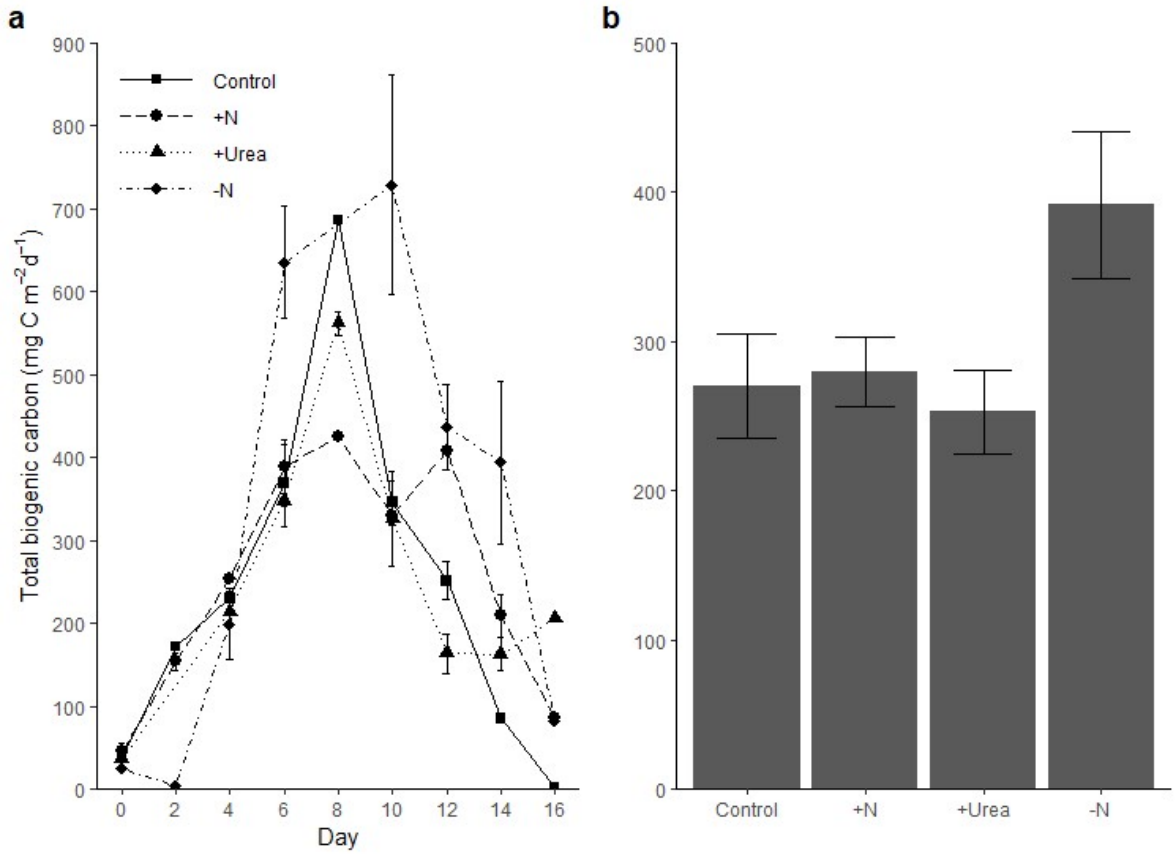

Figure 13. Temporal variations (a) and mean integrated values (b) of averaged downward fluxes of total biogenic carbon for the control, +N, +Urea and –N treatments. The error bars represent the standard error of 2 replicated measurements. There is no significant difference between treatments ($p > 0.05$)

4 DISCUSSION

4.1 Nutrients and microbial biomass

The nutrients were rapidly consumed in all mesocosms during the first two days of the experiment. This was probably caused by surge uptake by the nutrient-limited

phytoplankton, notably diatoms (Collos et al. 1997), which followed the enrichment of the mesocosms 12 h before the beginning of sampling. Despite this early nutrient depletion in the mesocosms, nanophytoplankton biomass continued to increase, reaching its maximum only at day 6. As in other coastal environments, phytoplankton cells of the Lower St. Lawrence Estuary, which is dominated by centric diatoms, accumulate nitrate and ammonium in their vacuoles during the spring bloom (Fauchot et al. 2000). This internal nitrogen pool can be used later for growth when ambient concentrations are decrease (Dortch, 1982).

Nitrate, phosphate and silicic acid were depleted after 2-3 days, whereas nitrite, ammonium and urea remained available at low concentrations in the mesocosms until the end of the experiment. This indicates nitrogen regeneration by bacterial, protistan or metazoan activities throughout the study. In contrast to the other nutrients, urea was never depleted, remaining at concentration > 0.2 µM. This lack of urea depletion was also observed during other mesocosm studies involving microplanktonic communities in the Lower St. Lawrence Estuary during mid-summer and surface waters of the Gulf of St. Lawrence during spring, summer and fall (Fauchot et al. 2000, Tremblay et al. 2000, Fouilland et al. 2003). During these studies, urea remained > 0.4 µM and > 0.2 µM. This may indicate that urea's phytoplankton affinity is lower than for the other nutrients or its regeneration is constantly higher than its utilization by phytoplankton. The half-saturation constant (K_s) for nitrate, ammonium and urea uptake averages 0.4 µM (Cochlan & Harrison 1991) for small oceanic diatoms and picophytoplankton. During the mesocosm experiment, the phytoplankton community > 4 µm was numerically dominated by the chain-forming centric diatom *Skeletonema costatum*. This species forms large blooms under conditions of cool temperature (< 20°C), high NO_3 concentration (> 10 µM), and turbulent mixing (Lomas & Glibert 2000, Fouilland et al. 2003). The maximum specific uptake rate (V_{max}) and K_s for this species are 0.12 h^{-1} and 0.5 µM for urea-deplete (McCarthy 1972) and 0.015 h^{-1} and 1.4 µM for urea-replete (Horrigan & McCarthy 1981, Antia et al. 1991)

cultures. These urea-affinity parameter values appear to be suitable for the natural diatom community of the St. Lawrence Estuary.

The various treatments had significant effects on particulate organic nitrogen and pigment concentrations, and nanophytoplankton carbon biomass. For all treatments, the picophytoplankton dynamics seemed influenced by heterotrophic nanoflagellates predation. The grazing pressure appears higher in nitrogen-enriched treatments. The sinking rates of free-living bacteria and picophytoplankton were low compared to those of particle-attached bacteria and nanophytoplankton. Since the picophytoplankton carbon biomass remained relatively low throughout the experiment, its vertical flux was negligible, except perhaps for particle-attached bacteria. The statistical analyses did not find any significant difference between treatments for TEP concentration. These exudates are an important carbon source for particle-attached bacteria, as reflected by a positive correlation between particle-attached bacteria and TEP(Fig. S2). Particle-attached bacteria have been shown to significantly contribute to nutrient remineralization (Bar-Zeev et al. 2009), explaining the NO_2 and NH_4 remineralization constantly observed throughout the experiment.

4.2 Potential effects of river input (+N treatment)

Waters of the St. Lawrence River contribute from 15 to 50% of the Lower St. Lawrence Estuary total nitrogen input (Gilbert et al. 2007). In a recent box-model, Jutras et al. (2020b) assumed a riverine contribution of 31% in summer. In the present study, a conservative 27% nitrate enrichment of the oceanic environment resulted in a significant increase in phytoplankton biomass. Therefore, the usual nutrient input from the St. Lawrence River itself may have a larger impact on phytoplankton biomass than observed in the mesocosms.

The input of dissolved nitrate led, on average, to a 24% increase in PON and a 13% increase in BSi, in proportion to the ratio in the Lower St. Lawrence Estuary, but deviating

from the critical Si:N molar ratio of diatoms of 0.9 (Brzezinski 1985). The nitrate consumption rate in the +N treatment (7.22 μM d^{-1}) was within the range of nitrate uptake rates (from 3.25 to 17.15 μM d^{-1}) measured during a phytoplankton spring bloom in the transition zone of the Lower Estuary to the Gulf of St. Lawrence (Tremblay et al. 2000). Hence, a bloom similar to that of the natural environment was induced in the mesocosms. During the late spring-early summer bloom, maximum chl *a* concentrations ~ 20 μg L^{-1} were observed in the Lower St. Lawrence Estuary (Levasseur & Therriault 1987, Annane et al. 2015). Maximum chl *a* concentrations were ~ 23 μg L^{-1} in the +N treatment indicating that the induced bloom had a similar biomass in the +N treatment than in the natural environment. In a different mesocosm experiment with natural microbial communities of the Lower St. Lawrence Estuary, Bénard et al. (2018) observed chl *a* concentrations similar to those observed in the present study with a maximum chl *a* concentrations ~ 27 μg L^{-1} on the third day of their experiment. In the +N treatment, nanophytoplankton carbon biomass, mainly composed of *S. costatum*, increased by 29% while chl *a* concentrations were on average 62% higher following the input of nitrogen. Previous studies have shown that if nitrogen is added to N-limited phytoplankton cells, the chl *a* content of the cells will increase almost immediately, although there may not be a corresponding response in cell growth or division (Rhee 1978, Lagus et al. 2004).

Although phytoplankton biomass increased in the +N treatment, the composition of the phytoplankton community remained the same as in the control, consisting of a majority of centric diatoms (~ 80%) and *S. costatum* (60%) specifically. This species which is common and abundant in the St. Lawrence Estuary (Bérard-Therriault et al. 1999), is often recorded in coastal waters around the world (Kooistra et al. 2008). Distinct N:P and Si:N ratios in the +N treatment did not reflect into a phytoplankton taxonomic composition shift, contrary to what might have been expected based on previous studies. In their review, Pinckney et al. (2001) discuss how an addition of dissolved inorganic nitrogen modifying the N:P and Si:N ratios promotes the proliferation of nuisance/toxic phytoplankton species

of dinoflagellates (e.g., *Alexandrium catenella* formely *A. tamarense*) and cyanobacteria (e.g., *Microcystis* spp.). It is possible that our experiment was too short to observe a shift in phytoplankton composition or that the dominance of *S. costatum* inhibited the proliferation of other species through the secretion of allelopathic substances (Wang et al. 2017).

Recently, Pinckney et al. (2020) estimated the concentration at which there is a fundamental change in phytoplankton communities in response to further increases in nutrient loading. They estimated that dissolved inorganic nitrogen thresholds are 25 and 50 μM for a high- and low-salinity estuaries, respectively. The threshold value has not been observed yet in the saline Lower St. Lawrence Estuary, but is close to it in the brackish and turbid waters of the Upper Estuary (Villeneuve 2020). Also, chl *a* concentrations are commonly used to designate desired endpoints for aquatic community structure and function, and regulatory criteria. For water quality management, typical thresholds are set at > 20 μg chl *a* L^{-1} (Pinckney et al. 2020), a concentration that has been reached during our experiment.

Although the temporal patterns of TEP were similar in the +N treatment and control, the maximum mean integrated concentration was in average 20% higher in the +N treatment. Maximum chl *a* concentrations occurred during the first three days of the experiment while maximum TEP concentrations occurred after 14 days. TEP concentrations were higher than those usually observed following the spring bloom in the St. Lawrence Estuary, and were similar to maximum values previously observed at the end of summer (Annane et al. 2015). TEP are a major source of carbon produced by phytoplankton and bacteria, mainly when nutrients become limited after the bloom (Passow et al. 2001), explaining the maximum TEP concentrations observed towards the end of the experiment. The diatom *S. costatum* has been reported to produce these exopolymeric substances in the Lower St. Lawrence Estuary (Annane et al. 2015), supporting that the enhanced TEP production in the present study could be mainly associated with this abundant species.

In this study, the sinking velocity of nanophytoplankton varied between 0 and 0.5 m d^{-1} with maxima around day 8 and 10, and minima at day 16. For *S. costatum* cultures, Bienfang et al. (1982) measured average sinking velocities of ~ 0.2, ~ 0.3 and ~ 0.1 m d^{-1} under conditions of recovery from nitrate depletion (24 h after an addition of nitrate to a nutrient-deplete diatom), nitrate repletion (= log-phase growth) and nitrate depletion (48 h without nitrate), respectively. In both studies, the algal cell buoyancy responded similarly to the nutrient regime change, with the lowest sinking velocities under nitrate depleted conditions.

Using SETCOL, Lapoussière et al. (2011) also reported sinking velocities similar to the present study for chl *a* (~ 0.25 m d^{-1}), diatoms (~ 0.36 m d^{-1}), flagellates (~ 0.26 m d^{-1}), particle-attached bacteria (~ 0.17 m d^{-1}) and free-living bacteria (~ 0.02 m d^{-1}) in the nitrogen-limited surface waters of Hudson Bay during late the summers of 2005 and 2006.

Annane et al. (2015) already observed that TEP, intact phytoplankton cells, pheopigments (as a proxy of senescent algal cells and fecal pellets) and heteroflagellates contributed most to carbon biomass in all treatments. Downward carbon fluxes of chl *a* and nanophytoplankton were on average 107 and 22% higher in the +N treatment than in control. The chl *a* carbon fluxes are overestimated comparatively to the nanophytoplankton because of the high chl *a* cellular content at the beginning of the experiment. Despite similar phytoplankton sinking speeds in the +N and control treatments, enhanced carbon biomass led to maximum mean integrated phytoplankton carbon flux under nitrate-enriched conditions. Hence, as a larger amount of phytoplankton potentially sinks toward the sea floor under nitrate-enriched conditions, an additional river input of nitrate as moderate as 27% in the Lower St. Lawrence Estuary would lead to enhanced phytoplankton export that may contribute to the removal of oxygen in the deepwater layers.

Downward fluxes of total biogenic carbon measured in the +N treatment and control were in the higher range of values (48 to 425 mg m^{-2} d^{-1}) observed in the Lower Estuary during the summer of 1993 (Romero et al. 2000). As the concentrations of chl *a*, and

nanophytoplankton and TEP were higher in the mesocosms than in the natural environment, it could explain why the carbon flux values were higher than the highest values previously reported in the Lower Estuary (Romero et al. 2000).

4.3 Enhanced fertilizers and waste release (+Urea treatment)

Urea is a form of organic nitrogen used in fertilizers and released from urban waters that ends up in coastal systems (Glibert et al. 2006, 2020). To support the increase in population and the required food supply, it is projected that global use of nitrogen fertilizer, which has increased about 9-fold since 1970, will continue to rise, and specifically that of urea will double by the year 2050 (Heffer and Prud'homme 2008, Glibert et al. 2020). Nearly 60% of all nitrogen fertilizer now used worldwide is in the form of urea (Constant & Sheldrick 1992,Glibert et al. 2006, 2020, 2014a, IFA 2020).One of the advantages of urea over ammonium nitrate (NH_4NO_3) is that the former is less explosive, therefore less dangerous for the farmers to handle. In Canada, urea represented ~ 15% of total nitrogen fertilizer used in 1970' and ~ 50% in 2018 (IFA 2020).

Organic nitrogen can be assimilated by diatoms, flagellated cells and some bacteria (Jørgensen 2006, Middelburg & Nieuwenhuize 2000). The +Urea treatment was specifically designed to mimic the replacement of nitrate by urea as a fertilizer and to determine the potential impact of this practice on the phytoplankton composition, biomass and sinking rate in the St. Lawrence marine system.

In our experimental study, the initial urea concentration in the +Urea treatment was 2.5 µM which is higher than those observed in the Lower St. Lawrence Estuary surface waters in mid-summer (i.e. ~ 0.4-1 µM; Fauchot et al. 2000, Fouilland et al. 2003) although levels up to 4 µM have been reported in the Gulf of St. Lawrence during fall (Tremblay et al. 2000). These concentrations are in the range of values reported in other estuaries (< 4 µM) but much lower than values measured in severely enriched waters such as

Chesapeake Bay (> 10 µM) and Chinese coastal waters (up to 20 µM) (Antia et al. 1991, Glibert et al. 2006).

During the first two days of the experiment, nitrate was consumed in proportion of its availability in all treatments. In contrast, the other nitrogenous nutrients (i.e. nitrite, ammonium and urea) were used in proportion lower than their availability. These results agree with those of Tremblay et al. (2000), showing that a phytoplankton community dominated by large phytoplankton tends to "prefer" nitrate over urea. However, the relative preference index for urea (0.899) was close to the one for nitrate (1.050) in the +Urea treatment. This means that the more urea there was in the environment, the more the microbial community used it. This implies that for the +Urea treatment, initial urea concentration was greater than the K_s threshold value for this nutrient.

A higher initial concentration of urea had no significant effect on the taxonomic composition of the phytoplankton community. As mention before, the diatom *S. costatum* typically dominates the phytoplankton community in the St. Lawrence Estuary during summer (Roy et al. 1996) and its presence is often linked to nitrogen-rich environments (Lomas & Glibert 2000). In their review on urea in coastal waters around the world, Glibert et al. (2006) noted a positive correlation between N-urea concentrations and the growth of cyanobacteria and dinoflagellates, but these two groups are generally in low abundance in the Lower St. Lawrence Estuary (Annane et al. 2015) and were scarce in the mesocosms. It is possible that urea concentrations were insufficient to favor the development of other phytoplanktonic groups, or that the potential release of an allelopathic substance by *S. costatum* affected their development (Wang et al. 2017) as indicated before. Even with a lower K_s for nitrate than for N-urea, *S. costatum* has been found to prefer urea in cultures containing concentrations of 2 µM for NO_3, NH_4 and N-urea (Huang et al. 2020). This centric diatom can therefore remain competitive over other phytoplankton groups in an environment enriched with 1.72 µM of N-urea as in our experiment. As *S. costatum* is strongly associated with TEP production and dominated in all treatments, it is not

surprising that the vertical carbon fluxes of the +Urea treatment were similar to those obtained for the +N treatment.

4.4 Reduced nitrogen river inputs (–N treatment)

We examined the potential impact of a 50% reduction in the river supply of dissolved nitrogen of anthropogenic origin through legislative efforts on the coastal waters of the St. Lawrence. In this hypothetical scenario, the –N treatment received approximately the same nitrogen concentration as the control, but the ΣN:P and ΣN:Si ratios differed, since we assumed no change in phosphate and silicic acid inputs from the river.

Under the reduced nitrogen river input scenario, the nitrate consumption rate during the two first days of the experiment was similar to the control, whereas the phosphate and silicic acid consumption rates remained similar to the two nitrogen-enriched treatments (Table 3). This indicates an enhanced uptake of silicic acid compared to total dissolved nitrogen in the –N treatment (Table 4). Furthermore, the diatom-specific consumption rate of silicic acid during the two first days of the experiment (Table 4) and the BSi:PON ratios from day 2 onwards were higher in the –N treatment than the other treatments (Fig. S3). As this ratio was above 0.9, the –N treatment was not limited in silicic acid. These results showed that a reduced input in dissolved nitrogen from the St. Lawrence River may enhance the silicification of the cell wall (frustule) of the diatom *S. costatum* and possibly *Chaetoceros* spp. in the Lower Estuary. Limitation of growth by factors other than silicon (i.e., light, nitrate or other elements) is often inversely correlated with silicification because a decrease in the growth rate gives a cell more time to acquire dissolved silicon (Claquin et al. 2002). Harrison et al. (1977) have shown that N-limitation and starvation change the silica and nitrogen content in *S. costatum* and *Chaetoceros debilis* increasing the BSi:PON molar ratios by 138% and 100-260%, respectively. Also, since nitrogen is the limiting nutrient for phytoplankton growth in the Lower St. Lawrence Estuary, it explains why the

reduced river input of nitrogen yielded to non significant different chl *a* and nanophytoplankton carbon biomass compared the unenriched oceanic control but higher BSi:PON ratio (Table 6).

The lower proportion of pheopigment concentrations relative to chl *a* suggests a reduced grazing pressure by heterotrophic organisms under the –N treatment compared to the other treatments, possibly due to the enhanced silicification of diatoms. Studies that measured changes in grazing pressure with silicification changes found that increasing silicification led to decreased predation from microzooplankton (Zhang et al. 2017) and copepods (Liu et al. 2016).

Silicification also increases the mass density of the frustule and can affect the rate at which cells sink (Raven & Waite 2004). During the experiment, the sinking velocities of total pigments and nanophytoplankton were, on average, high in the –N treatment compared to the other treatments (including the control); the percent increase being 47% and 75% for these two variables, respectively. Enhanced BSi production could have increased diatom mass density and therefore, the ballast of the cell (Krause et al. 2019). In the natural environment, higher mass density of diatoms allow them to descend at depths where nutrients are more available (Raven & Waite 2004). The sinking fluxes of nanophytoplankton were 101% higher in the –N treatment than in the control, probably due to the enhanced silicification of centric diatoms when less limited in silicic acid. These results are consistent with those of a previous microcosm study on the silicification of diatoms in northwest coastal waters of the United States (Durkin et al. 2013). As in our study, a higher seawater Si:N ratio led diatom communities to produce more BSi which doubled their sinking speeds. Hence, changes in silicification did not only affected energy flows through the food web but also the downward fluxes of the diatoms community.

4.5 The effect of cell size and grazing on residence times

The residence time of particles in the mesocosms was estimated with their concentration reported to their downward flux multiplied by the mesocosm height (Table 7). As expected, pico-sized particles such as picophytoplankton and free-living bacteria showed the most extended residence times ranging from 6.4 to 11 days and from 13.9 to 99 days, respectively. For the larger particles, the residence times were shorter (~ 2-3 days). The longest residence times were generally observed in the two most nitrogen-enriched treatments. However, the residence times of most large particles were shorter in the –N treatment than in the other treatments. In this study, large zooplankton grazers

Table 7. Estimated residence time in days for different biological variables studied. Minimal values are in bold

	Control	**+N**	**+Urea**	**–N**
Chlorophyll *a*	2.1	1.6	1.9	**1.5**
Pheopigments	1.9	1.9	2.0	**1.3**
Total pigments	2.0	1.7	1.7	**1.5**
Picophytoplankton	10.4	**6.4**	8.1	11.0
Nanophytoplankton	2.0	2.1	2.2	**1.2**
Heterotrophic nanoflagellates	4.0	6.3	6.1	**2.8**
Free-living bacteria	**13.9**	46.5	14.6	99.0
Particle-attached bacteria	2.2	2.1	3.7	**2.0**
TEP	2.5	3.1	2.6	**1.7**
Total biogenic carbon and TEP	2.0	2.4	2.6	**1.5**

producing fast sinking fecal pellets were removed at the beginning of the experiment. Their presence would have changed the structure of the phytoplankton community and most probably enhanced the sinking export of the large phytoplankton. Overall, these results indicated that the downward fluxes of particles were driven by multiple factors, including particle size, mass density and grazing activity.

5 CONCLUSIONS

By characterizing the composition and vertical fluxes of the microbial community in the Lower St. Lawrence Estuary under different nitrogenous nutrient concentrations, this study has shown that river nitrogen inputs promote microbial growth and accumulation. However, a higher proportion of urea in river inputs did not favor the proliferation of potentially toxic phytoplankton species. Instead, the centric diatom *S. costatum* dominated the phytoplankton community in all treatments, leading to high downward carbon fluxes. The fluxes were especially elevated under a 50% reduction in nitrogen availability due to enhanced silicification of the diatom cells. Therefore, a simple decrease in nitrogenous nutrient inputs of fertilizers and waste releases in the St. Lawrence River may not lead to a reduction in downward carbon fluxes.

As the experiment was carried out in mesocosms in the absence large zooplankton, several additional questions must be considered before applying the results to the natural environment of the Lower St. Lawrence Estuary. In an environment where there is more organic matter as in the +N and +Urea treatments, this could lead to an increase in grazing by zooplankton and therefore in fecal pellets production. According to Genin et al. (2021), fecal pellets represented up to 64% of total downward fluxes of biogenic carbon the carbon fluxes in the Gulf of St. Lawrence during the spring bloom. In nitrogen poor environment (i.e., –N treatment), diatoms were less abundant, more silicified, and remained suspended in

suspension in the water column for a short period. Under these conditions, Liu et al. (2016) showed that large zooplankton may have a lesser impact on the carbon sinking fluxes.

Having been tested only over one bloom period, it is not possible to conclude if similar results would be observed over a longer period. Possible scenarios could be simulated by biogeochemical models. By isolating the effect of river nitrogen inputs on microbial communities, these results are highly useful and relevant for these models and future projections of vertical carbon fluxes. An increasing use of urea may potentially have different effects over several years. A return to pre-eutrophication environmental conditions rarely occurs linearly following a reduction in nutrients (Carstensen et al. 2011). For coastal waters, it takes on average 15 years to return to non-eutrophic conditions following a complete reduction and on average 31 years following a partial reduction in nutrients (McCrakin et al. 2017). A regulation of nitrogenous nutrient releases should certainly take into account the concentrations and ratios of nutrients potentially promoting the growth of phytoplankton and the presence of toxic dinoflagellates and cyanobacteria. Natural levels of silicic acid in the environment may also vary over the next few years depending on the changing runoff levels due to climate change (Lavoie et al. 2020). Silicic acid and upwelled nitrogen and phosphorous are less manageable than nutrients from anthropogenic sources. Environmental control measures concerning the Lower St. Lawrence Estuary should aim for nutrient ratios that take into account these other sources of nutrients and limit as much as possible the amount of carbon that can be exported and decomposed in deep layers already showing signs of damage by eutrophication.

CONCLUSION GÉNÉRALE

Les apports fluviaux en nutriments azotés sont responsables de l'eutrophisation des eaux côtières à l'échelle globale. Dans ce contexte, il est important de déterminer les effets d'un changement de ces apports sur les communautés microbiennes et leurs flux verticaux. La couche profonde de l'estuaire maritime du Saint-Laurent présente des symptômes d'eutrophisation, tels que des concentrations en oxygène dissous inférieures au seuil d'hypoxie et une acidification du milieu persistants à l'année longue (Gilbert et al. 2007; Mucci et al. 2011). C'est pour mieux comprendre ce phénomène que le réseau de recherche SECO.Net a été mis sur pied en 2017.

L'article intégré dans ce mémoire de maîtrise porte sur une étude en mésocosmes qui s'insère dans le volet expérimental du projet. L'objectif était de tester l'influence des apports fluviaux en azote sur la composition et les flux verticaux de la communauté microbienne de l'estuaire maritime du Saint-Laurent. Trois scénarios réalistes y ont été testés : un actuel (+N) recréant la rencontre entre les eaux de remontée de l'estuaire maritime et celles de l'estuaire fluvial du Saint-Laurent; un futuriste (+Urée) avec un apport plus important en urée; et un de remédiation (–N) où les apports fluviaux en nitrate sont réduits de 50% grâce, entre autres, à des mesures législatives.

Les résultats de l'étude ont montré que les apports fluviaux en nutriments azotés accroissent les concentrations en azote organique particulaire (PON), en chlorophylle *a* (chl *a*) ainsi que la biomasse carbonée du nanophytoplancton (> 2 μm) dans l'estuaire maritime du Saint-Laurent. Ce résultat soutient l'hypothèse de travail soutenant que les apports en azote favorise une communauté microbienne abondante. La diatomée centrale *Skeletonema costatum* a dominé la communauté phytoplanctonique dans tous les traitements tout au long de l'expérience. Cette espèce présente une morphologie et une taille (3-16 μm) très variables (Bérard-Therriault et al. 1999). Aucune espèce nuisible a été

observée dans les mésocosmes enrichis en urée. Ce résultat ne soutient pas la seconde hypothèse de ce travail voulant qu'une augmentation des apports en urée favoriserait à court terme la floraison d'algues nuisibles ou toxiques dans l'estuaire maritime du Saint-Laurent.

La réduction des apports en nitrate a entraîné, en général, une baisse des concentrations en PON, mais la concentration en BSi est restée sensiblement la même que dans les traitements enrichis en azote. Ces résultats indiquent que les diatomées dans les mésocosmes simulant un scénario de remédiation avaient un ratio BSi:PON plus élevé. La diminution des apports en NO_3 par rapport au $Si(OH)_4$ dans ces mésocosmes a sans doute favorisé la silicification des diatomées ce qui a en moyenne accru l'intensité des flux verticaux descendants moyens. La silicification accrue des diatomées semble avoir également diminué le broutage sur ces cellules, car le rapport entre les phéopigments et les pigments totaux y est plus élevé.

Cette expérience a également permis de montrer que la réponse du bactérioplancton et du picophytoplancton eucaryote (≤ 2 µm) aux apports fluviaux en nutriments est différente de celle du nanophytoplancton. La dynamique du picophytoplancton est fortement influencée par le broutage par les flagellés hétérotrophes. La pression de broutage semble plus élevée dans les mésocosmes fortement enrichis en azote dissous. La dynamique des bactéries libres semble quant-à-elle être gouvernée par le broutage et potentiellement par les infections virales (non présentées ici) tandis que celle des bactéries attachées aux particules est fortement associée aux variations des concentrations en TEP. Les vitesses de chute des bactéries libres et du picophytoplancton sont faibles par rapport à celles des bactéries attachées aux particules et au nanophytoplancton. Puisque la biomasse carbonée du picophytoplancton reste relativement faible tout au long de l'expérience, leur flux vertical est négligeable, sauf peut-être pour les bactéries attachées aux particules.

Cette expérience a été réalisée avec une communauté planctonique naturelle provenant de l'estuaire maritime du Saint-Laurent. La communauté a été soumise à des conditions de lumière naturelle, à une température constante de 8°C proche de celle du milieu naturel en été et à un mélange vertical constant assuré par une hélice qui tournait à 10 cm/s. Les mésocosmes ont été enrichis à des concentrations réalistes en nutriments une

seule fois au début de l'expérience comme si une masse d'eau de remontée rencontrait les eaux fluviales et était par la suite advectée. Toutefois, il faut être prudent quant à l'extrapolation des résultats obtenus en milieu contrôlé par rapport aux conditions dans le milieu naturel. Au cours de cette expérience, le macrozooplancton (> 300 µm) a été retiré au début de l'expérience. La présence de macrozooplancton dans un environnement chargé en matière organique ayant un temps de résidence de plusieurs jours pourrait conduire à un broutage important. Les pelotes fécales produites par le macrozooplancton peuvent représenter une part importante des flux verticaux en carbone dans les milieux marins en général et l'estuaire du Saint-Laurent en particulier (Roy et al. 2000, Genin et al. 2021).

L'augmentation graduelle des apports en nutriments dans le milieu naturel pourrait avoir des effets à long terme différentes de ceux observés au cours de notre expérience en mésocosmes. Dans le contexte des changements climatiques, il serait intéressant d'étudier si des changements dans les apports de l'azote inorganique et organique dissous et du silicium dissous pourraient favoriser la croissance d'espèces nuisibles ou toxiques ou de nouvelles espèces dans le système marin du Saint-Laurent.

Notre étude en mésocosmes nous a permis de mieux comprendre l'influence des apports fluviaux en azote sur les premiers échelons trophiques de l'estuaire du Saint-Laurent. Elle a été réalisée sous des conditions de température et de turbulence constantes simulant celles du milieu naturel et en présence de brouteurs planctoniques (< 300 µm). Les résultats présentés dans le cadre de cette étude seront hautement pertinents pour le volet concernant la modélisation biogéochimique du projet SECO.Net.

INFORMATIONS SUPPLÉMENTAIRES

Table S1. Summary of one-way ANOVA or Kruskall-Wallis to seek differences between treatments for nutrient consumption rates. Values significantly different between treatments (p-value < 0.05) were subjected to a post-hoc Tukey HDS test (a > b > c > d)

				Tukey			
Variable	Statistical analysis	Transformation	p-value	Control	+N	+Urea	–N
ρNO_3	one-way ANOVA		< 0.001	c	a	b	c
ρNO_2	one-way ANOVA		0.248				
ρNH_4	one-way ANOVA	log	0.096				
ρN-urea	Kruskall-Wallis		0.027	b	b	a	b
ρPO_4	one-way ANOVA		0.034	a	a	a	a
$\rho Si(OH)_4$	Kruskall-Wallis		0.075				

Table S2. Summary of one-way ANOVA to seek differences treatments for nutrient consumption ratios. Values significantly different between treatments (p-value < 0.05) were subjected to a post-hoc Tukey HDS test (a > b > c > d)

		Tukey			
Variable	p-value	Control	+N	+Urée	–N
ρNO_3:ρPO_4^3	< 0.001	c	a	b	c
ρNO_3:$\rho Si(OH)_4$	< 0.001	a	a	b	c
ρTDN: ρSi	< 0.001	b	ab	a	c
$\rho Si(OH)_4$/ρBSi	0.157				
$\rho Si(OH)_4$/diatom	0.426				

Table S3. Summary of one-way ANOVA to seek differences between treatments for the relative preference index (RPI) of nitrogenous nutrients. There was no significant difference between treatments (p > 0.05)

RPI	Transformation	p-value
Nitrate	log	0.383
Nitrite		0.094
Ammonium		0.242
N-urée		0.147

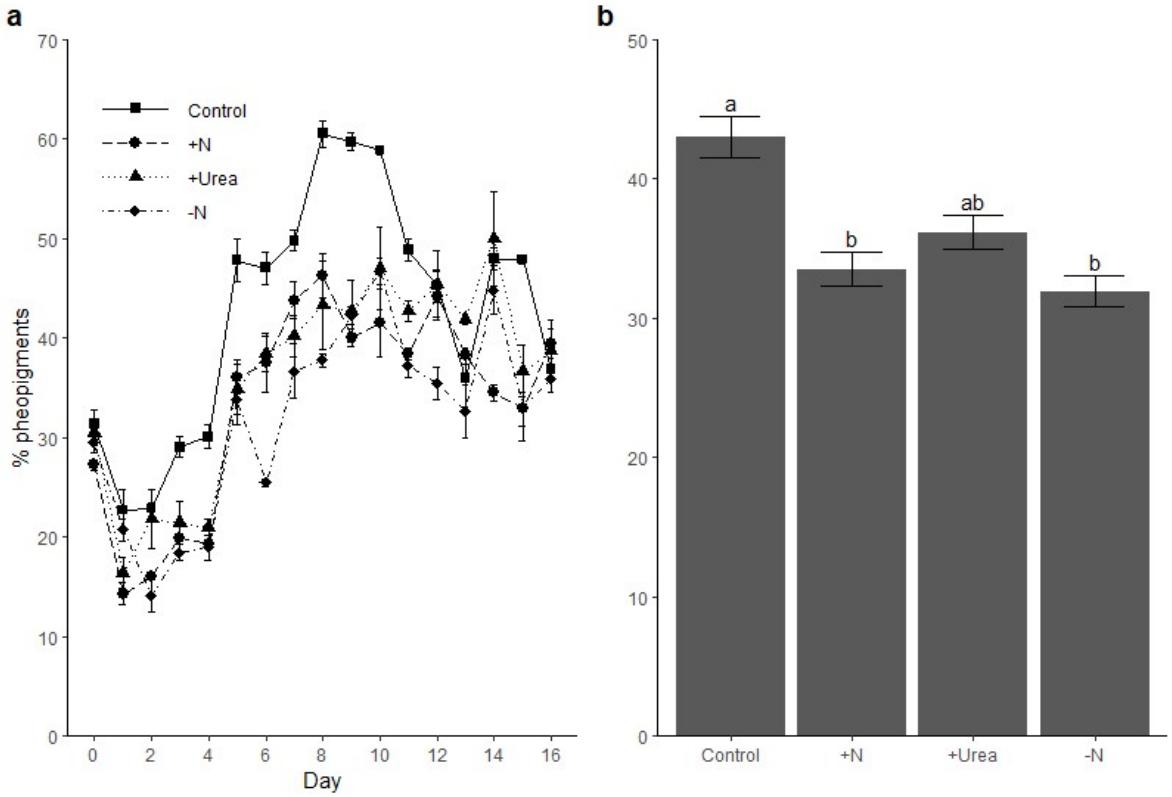

Figure S1. Temporal variations (a) and integrated means over time (b) of the percentage of pheopigments in relation to the concentration of total pigments for the control, +N, +Urea and –N treatments. The error bars represent the standard error of three replicated measurements. There was a significant difference between treatments ($p < 0.05$) and Tukey post-hoc test denoted two groups (a > b).

Table S4. Summary of linear mixed effects model (lmem) for different biological variables studied (concentrations ~ treatments | days). Values significantly different between treatments (p-value < 0.05) were subjected to a post-hoc Tukey test (a > b > c > d)

Concentration	**lmem**	**Tukey (a > b > c > d)**			
	(p-value)	**Control**	**+N**	**+Urea**	**–N**
Chlorophyll *a* (µg L^{-1})	< 0.001	b	a	a	b
Pheopigments (µg L^{-1})	sqrt < 0.01	a	a	a	b
Total pigments (µg L^{-1})	< 0.001	b	a	a	b
PON (µM)	< 0.001	b	a	a	b
POP (µM)	0.332				
BSi (µM)	0.171				
Picophytoplankton (µg C L^{-1})	0.250				
Nanophytoplankton (µg C L^{-1})	0.014	b	a	a	ab
Heterotrophic flagellates (µg C L^{-1})	0.053				
Free-living bacteria (µg C L^{-1})	0.438				
Particle attached bacteria (µg C L^{-1})	0.021	a	a	a	a
TEP (µg C L^{-1})	0.258				
Total biogenic carbon (µg C L^{-1})	< 0.01	b	a	a	b
Sinking velocities (m d^{-1})					
Chlorophyll *a*	0.802				
Pheopigments	0.840				

Total pigments	sqrt 0.848
Picophytoplankton	0.674
Nanophytoplankton	sqrt 0.875
Heterotrophic nanoflagellates	0.843
Free-living bacteria	0.521
Particle-attached bacteria	log 0.602
TEP	log 0.123
Downward fluxes (mg C m^{-2} d^{-1})	
Chlorophyll *a*	0.800
Pheopigments	0.950
Total pigments	0.910
Picophytoplankton	0.066
Nanophytoplankton	0.803
Heterotrophic nanoflagellates	0.880
Free-living bacteria	0.696
Particle-attached bacteria	0.814
TEP	0.342
Total biogenic carbon	0.986

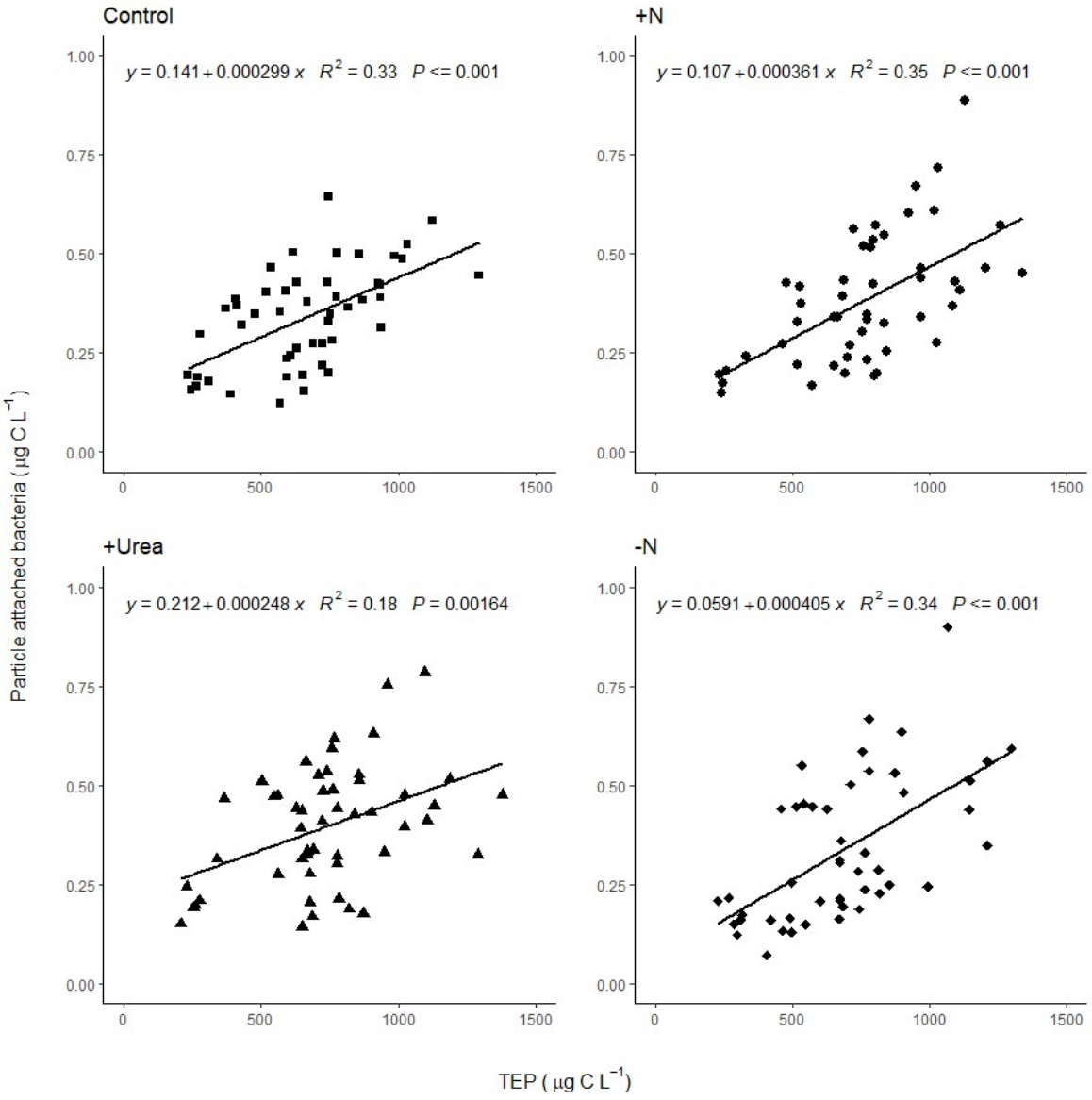

Figure S2. Linear regressions between particle-attached bacteria and transparent exopolymeric particles (TEP) for the control, +N, +Urea and –N treatments

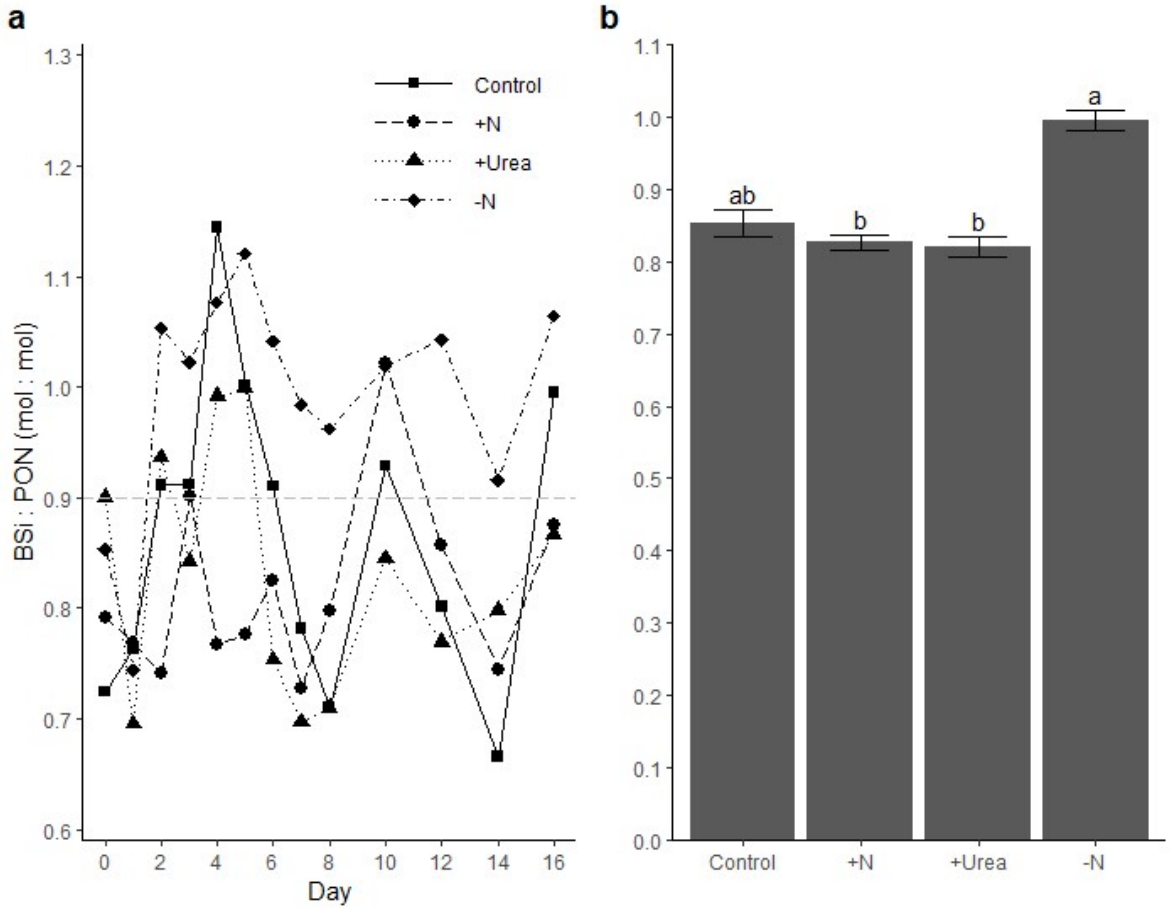

Figure S3. Temporal variations (a) and integrated means (b) of BSi:PON ratio for the control, +N, +Urea and –N treatments. The horizontal dotted gray line represents the BSi:PON ratio of Brzezinski (1985). The error bars represent the standard error of three replicated measurements. There is a significant difference between treatments ($p < 0.001$). The post-hoc Tukey test denotes two groups: a > b

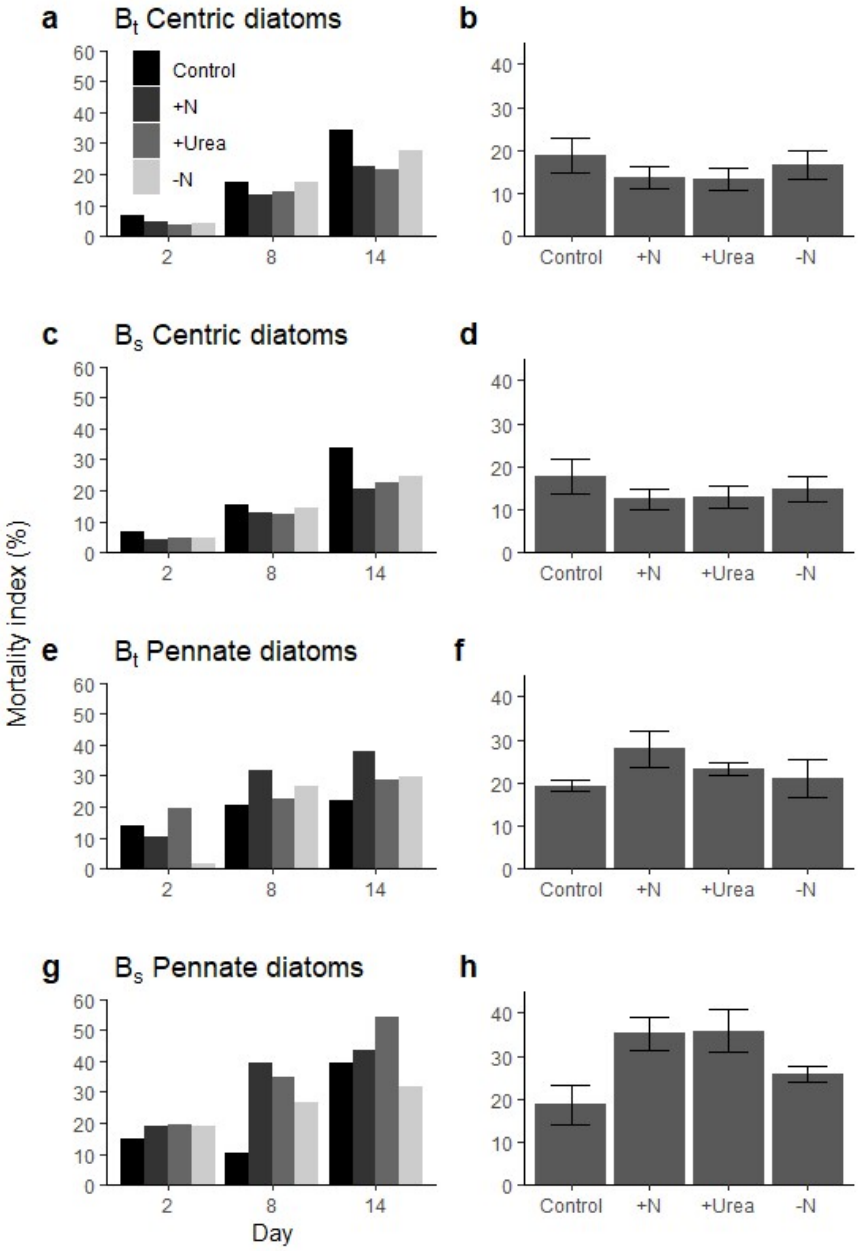

Figure S4. Variations and integrated means of the mortality index of a-d) centric and e-h) pennate diatoms measured in the samples from the control bottle (B_t) and bottom section of the settling column (B_s) on days 2, 8 and 14 for the control, +N, +Urea and –N treatments. The error bars represent the standard error of 2 replicated measurements. There was no significant difference between treatments ($p > 0.05$).

RÉFÉRENCES BIBLIOGRAPHIQUES

Anderson DM, Burkholder JM, Cochlan WP, Glibert P, Gobler CJ, Heil CA, Kudela RM, Parsons ML, Jack Rensel JE, Townsend DW, Trainer VL, Vargo GA (2008) Harmful algal blooms and eutrophication: Examining linkages from selected coastal regions of the United States. Harmful Algae 8:39-53

Annane S, St-Amand L, Starr M, Pelletier E, Ferreyra G (2015) Contribution of transparent exopolymeric particles (TEP) to estuarine particulate organic carbon pool. Mar Ecol Prog Ser 529:17-34

Antia NJ, Harrison PJ, Oliveira L (1991) The role of dissolved organic nitrogen in phytoplankton nutrition, cell biology and ecology. Phycologia 30:1-89

Azetsu-Scott K, Passow U (2004) Ascending marine particles: Significance of transparent exopolymer particles (TEP) in the upper ocean. Limnol Oceanogr 49:741-748

Barrera-Alba JJ, Gianesella SMF, Moser GAO, Saldanha-Corrêa FMP (2009) Influence of allochthonous organic matter on bacterioplankton biomass and activity in a eutrophic, sub-tropical estuary. Estuar Coast Shelf S 82:84-94

Bar-Zeev E, Berman-Frank I, Stambler N, Vázquez Domínguez E, Zohary T, Capuzzo E, Meeder E, Suggett DJ, Iluz D, Dishon G, Berman T (2009) Transparent exopolymer particles (TEP) link phytoplankton and bacterial production in the Gulf of Aquaba. Aquat Microb Ecol 56:217-225

Bénard R, Levasseur M, Scarratt M, Blais M-A, Mucci A, Ferreyra G, Starr M, Gosselin M, Tremblay J-E, Lizotte M (2018) Experimental assessment of the sensitivity of an estuarine phytoplankton fall bloom to acidification and warming. Biogeosciences 15:4883-4904

Benoit P, Gratton Y, Mucci A (2006) Modeling of dissolved oxygen levels in the bottom waters of the Lower St. Lawrence Estuary: Coupling of benthic and pelagic processes. Mar Chem 102:13-32

Bérard-Therriault L, Poulin M, Bossé L (1999) Guide d'identification du phytoplancton marin de l'estuaire et du golfe du Saint-Laurent : incluant également certains protozoaires. Publ spéc can sci halieut aquat. 128:387 p

Bienfang PK (1981) SETCOL – A technologically simple and reliable method for measuring phytoplankton sinking rates. Can J Fish Aquat Sci 38:1289-1294

Bienfang PK, Harrison PJ, Quarmby LM (1982) Sinking rate response to depletion of nitrate, phosphate and silicate in four marine diatoms. Mar Biol 67:295-305

Bienfang P, Szyper J, Laws E (1983) Sinking rate and pigment responses to light-limitation of a marine diatom-implications to dynamics of chlorophyll maximum layers. Oceanol Acta 6:55-62

Bricker SB, Clement CG, Pirhalla DE, Orlando SP, Farrow DRG (1999) National estuarine eutrophication assessment: Effects of nutrient enrichment in the nation's estuaries.

NOAA, National Ocean Service, Special Projects Office and the National Centers for Coastal Ocean Service. Silver Spring MD, 71 p.
Brzezinski MA (1995) The Si:C:N ratio of marine diatoms: interspecific variability and the effect of some environmental variables. J Phycol 21:347-357
Buck K R, Newton J (1995) Fecal pellet flux in Dabob Bay during a diatom bloom: Contribution of microzooplankton. Limnol Oceanogr 40:306-315
Cai WJ, Hu X, Huang WJ, Murell MC, Lehrter JC, Lohrenz SE, Chou WC, Zhai W, Hollibaugh JT, Wang Y, Zhao P, Guo X, Gundersen K, Dai M and Gong CG (2011) Acidification of subsurface coastal waters enhanced by eutrophication. Nat Geosci 4:766-770
Carstensen J, Andersen JH, Gustafsson BG, Conley DJ (2014) Deoxygenation of the Baltic Sea during the last century. Proc Natl Acad Sci USA 111:5628-5633
Carstensen J, Duarte CM (2019) Drivers of pH variability in coastal ecosystems. Environ Sci Technol 53:4020-4029
Carstensen J, Sánchez-Camacho M, Duarte C, Krause-Jensen D, Marbà N (2011) Connecting the dots: Responses of coastal ecosystems to changing nutrient concentrations. Environ Sci Technol 45:9122:9132
Christaki U, Courties C, Massana R, Catala P, Lebaron P, Gasol JM, Zubkov MV (2011) Optimized routine flow cytometric enumeration of heterotrophic flagellates using SYBR Green I. Limnol Oceanogr: Meth 9:329-339
Claquin P, Martin-Jézéquel V, Kromkamp JC, Veldhuis MJW, Kraay GW (2002) Uncoupling of silicon compared with carbon and nitrogen metabolisms and the role of the cell cycle in continuous cultures of *Thalassiosira pseudonana* (Bacillariophyceae) under light, nitrogen, and phosphorus control. J Phycol 38:922-930
Claret M, Galbraith ED, Palter JB, Bianchi D, Fennel K, Gilbert D, Dunne JP (2018) Rapid coastal deoxygenation due to ocean circulation shift in the Northwest Atlantic. Nat Clim Change 8:868-872
Cloern JE (2001) Our evolving conceptual model of the coastal eutrophication problem. Mar Ecol Prog Ser 210:223-253
Cochlan WP, Harrison PJ (1991) Kinetics of nitrogen (nitrate, ammonium and urea) uptake by the picoflagellate *Micromonas pusilla* (Prasinophyceae). J Exp Mar Biol Ecol 153:129-141
Collos Y, Vaquer A, Bibent B, Slawyk G, Garcia N, Souchu P (1997) Variability in nitrate uptake kinetics of phytoplankton communities in a Mediterranean coastal lagoon. Estuar Coast Shelf S 44:369-375
Constant KM, Sheldrick WF (1992) World nitrogen survey. World Bank 215 p.
Cyr F, Bourgault D, Galbraith PS, Gosselin M (2015) Turbulent nitrate fluxes in the Lower St. Lawrence Estuary, Canada. J Geophys Res Oceans 120: 2308-2330
Diaz RJ, Rosenberg R (2008) Spreading dead zones and consequences for marine ecosystems. Science 321:926-929
Dorth, Q (1982) Effect of growth conditions on accumulation of internal nitrate, ammonium, aminoacids, and protein in three marine diatoms. J Exp Mar Biol Ecol 61:243-264

Durkin CA, Bender SJ, Chan KYK, Gaessner K, Grünbaum D, Armbrust EV (2013) Silicic acid supplied to coastal diatom communities influences cellular silicification and the potential export of carbon. Limnol Oceanogr 58:1707-1726

Engel A, Passow U (2001) Carbon and nitrogen content of transparent exopolymer particles (TEP) in relation to their Alcian Blue adsorption. Mar Ecol Prog Ser 219:1-10

Eppley RW, Peterson BJ (1979) Particulate organic matter flux and planktonic new production in the deep ocean. Nature 282:677-680

Fauchot J, Gosselin M, Levasseur M, Mostajir B, Belzile C, Demers S, Roy S, Villegas PZ (2000) Influence of UV-B radiation on nitrogen utilization by a natural assemblage of phytoplankton. J Phycol 36:484-496

Fouilland E, Gosselin M, Mostajir B (2003) Effects of ultraviolet-B radiation and vertical mixing on nitrogen uptake by a natural planktonic community shifting from nitrate to silicic acid deficiency. Limnol Oceanogr 48:18-30

Fuhrman JA (1999) Marine viruses and their biogeochemical and ecological effects. Nature 399:541-548

Gałecki A., Burzykowski T. (2013) Linear mixed-effects model. In *Linear Mixed-Effects Models Using R*. Springer, New York, pp. 245-273

Genin F, Lalande C, Galbraith PS, Larouche P, Ferreyra GA, Gosselin M (2021) Annual cycle of biogenic carbon export in the Gulf of St. Lawrence. Cont Shelf Res 221:104418

Gilbert D, Chabot D, Archambault P, Rondeau B, Hébert S (2007) Appauvrissement en oxygène dans les eaux profondes du Saint-Laurent marin: causes possibles et impacts écologiques. Le Naturaliste Canadien 31:67-75

Gilbert D, Rabalais N, Diaz R, Zhang J (2010) Evidence for greater oxygen decline rates in the coastal ocean than in the open ocean. Biogeosciences 7:2283

Gilbert D, Sundby B, Gobeil C, Mucci A, Tremblay GH (2005) A seventy-two year record of diminishing deep-water oxygen in the St. Lawrence estuary: The Northwest Atlantic connection. Limnol Oceanogr 50:1654-1666

Glibert P (2020) Harmful algae at the complex nexus of eutrophication and climate change. Harmful Algae. 91:101583

Glibert PM, Harrison J, Heil C, Seitzinger S (2006) Escalating worldwide use of urea – a global change contributing to coastal eutrophication. Biogeochemistry 77:441-463

Glibert PM, Maranger R, Sobota DJ, Bouwman L (2014) The Haber Bosch-harmful algal bloom (HB-HAB) link. Environ Res Lett 9:105001

Glibert PM, Seitzinger S, Heil CA, Burkholder JM, Parrow MW, Codispoti LA, Kelly V (2005) The role of eutrophication in the global proliferation of harmful algal blooms: New perspectives and new approaches. Oceanography 18:198-209

Goeyens L, Kindermans N, Yusuf M A, Elskens M (1998) A room temperature procedure for the manual determination of urea in seawater. Estuar Coast Shelf S 47:415-418

Granéli E, Wallström L, Larsson U, Granéli W, Elmgrem R (1990) Nutrient limitation of primary production in the Baltic Sea area. Ambio 19:142-151

Hansen HP, Koroleff F (1999) Determination of nutrients. In: Grasshoff K, Kremling K, Ehrhardt M (eds). Methods of seawater analysis, 3rd edn. Wiley-VCH, New York, NY, p 159-228

Harrison PJ, Conwey HL, Holmes RW, Davis CO (1977) Marine diatoms grown in chemostats under silicate or ammonium limitation. III. Cellular chemical composition and morphology of *Chaetoceros debilis*, *Skeletonema costaum*, and *Thalassiosira gravida*. Mar Biol 43:19-31

Harrison PJ, Zingone A, Mickelson MJ, Lehtimen S, Ramaiah N, Kraberg AC, Sun J, McQuatters-Gollop A, Jakobsen HH (2015) Cell volumes of marine phytoplankton from globally distributed coastal data sets. Estuar Coast Shelf S 162:130-142

Hecky RE, Kilham P (1988) Nutrient limitation of phytoplankton in freshwater and marine environments: a review of recent evidence on the effects of enrichment. Limnol Oceanogr 33:796-822

Heffer P, Prud'homme M (2008) Outlook for world fertilizer demand, supply, and supply/demand balance. Turk J Agric For 32:159-164

Holligan PM, Harris RP, Newell RC, Harbour DS, Head RN, Linley EAS, Lucas MI, Tranter PRG, Weekley CM (1984) Vertical distribution and partitioning of organic carbon in mixed, frontal and stratified waters of the English Channel. Mar Ecol Prog Ser 14:111-127

Holmes RM, Aminot A, Kérouel R, Hooker BA, Peterson BJ (1999) A simple and precise method for measuring ammonium in marine and freshwater ecosystems. Can J Fish Aquat Sci 56:1801-1808

Horrigan SG, McCarthy JJ (1981) Urea uptake by phytoplankton at various stages of nutrient depletion. J Plankton Res 3:403-414

Howarth RW, Billen G, Swaney D, Townsend A, Jaworski N, Lajtha K, Downing JA, Elmgren R, Caraco N, Jordan T, Berendse F, Freney J, Kudeyarov V, Murdoch P, Zhao-liang Z (1996) Regional nitrogen budgets and riverine inputs of N and P for the drainages to the North Atlantic Ocean: natural and human influences. Biogeochemistry 35:75-139

Howarth RW, Marino R (2006) Nitrogen as the limiting nutrient for eutrophication in coastal marine ecosystems: Evolving views over three decades. Limnol Oceanogr 51:364-376

Huang K, Feng Q, Zhang Y, Ou L, Cen J, Lu S, Qi Y. (2020) Comparative uptake and assimilation of nitrate, ammonium, and urea by dinoflagellate *Karenia mikimotoi* and diatom *Skeletonema costatum* s. l. in the coastal waters of the East China Sea. Mar Pollut Bull 155:111200

Hudon C, Gagnon P, Rondeau M, Hébert S, Gilbert D, Hill B, Patoine M, Starr M (2017) Hydrological and biological processes modulate carbon, nitrogen and phosphorus flux from the St. Lawrence River to its estuary (Quebec, Canada). Biogeochemistry 135:251-276

Hudon C, Jean M, Létourneau G (2018) Temporal (1970–2016) changes in human pressures and wetland response in the St. Lawrence River (Québec, Canada). Sci Total Environ 643:1137-1151

International Fertilizer Association (2020) http://ifadata.fertilizer.org/ucSearch.aspx

Jackson GA (1990) A model of the formation of marine algal flocs by physical coagulation processes. Deep-Sea Res 37:1197-1211

Jiang Q, He J, Wu J, Hu X, Ye G, Christakos G (2018) Assesing the severe eutrophication status and spatial trend in the coastal waters of Zhejiang Province (China). Limnol Oceanogr 64:3-17

Jørgensen NO (2006) Uptake of urea by estuarine bacteria. Aquat MicrobEcol 42:227-242

Jutras M, Dufour CO, Mucci A, Cyr F, Gilbert D (2020a) Temporal changes in the causes of the observed oxygen decline in the St Lawrence Estuary. J Geophys Res-Oceans 125: e2020JC016577, doi:10.1029/2020JC016577

Jutras M, Mucci A, Sundby B, Gratton Y, Katsev S (2020b) Nutrient cycling in the Lower St. Lawrence Estuary: Response to environmental perturbations. Estuar Coast Shelf Sci 239:106715

Krause JW, Schulz IK, Rowe KA, Dobbins W, Winding MHS, Sejr MK, Duarte CM, Agusti S (2019) Silicic acid limitation drives bloom termination and potential carbon sequestration in an Arctic bloom. Sci Rep-UK 9:1-11

Kooistra WHCF, Sarno D, Balzano S, Gu H, Anderson RA, Zingone A (2008) Global diversity and biogeography of *Skeletonema* species (bacillariophyta). Protist 159:177-193

Lagus A, Suomela J, Weithoff G, Heikkila K, Helminen H, Sipura J (2004) Species-specific differences in phytoplankton responses to N and P enrichments and the N:P ratio in the Archipelago Sea, northern Baltic Sea. J Plankton Res 26:779-798

Lapoussière A, Michel C, Starr M, Gosselin M, Poulin M (2011) Role of free-living and particle-attached bacteria in the recycling and export of organic material in the Hudson Bay system. J Mar Syst 88:434-445

Larsen JB, Larsen A, Thyrhaug R, Bratbak G, Sandaa R-A (2008) Response of marine viral populations to a nutrient induced phytoplankton bloom at different pCO_2 levels. Biogeosciences 5:523-533

Laurenceau-Cornec EC, Le Moigne FA, Gallinari M, Moriceau B, Toullec J, Iversen MH, Engel A, De La Rocha CL (2019) New guidelines for the application of Stokes' models to the sinking velocity of marine aggregates. Limnol Oceanogr 65:1264-1285

Lavoie D, Lambert N, Rousseau S, Dumas J, Chassé J, Long Z, Perrie W, Starr M, Brickman D, Azetsu-Scott K (2020) Projections of future physical and biogeochemical conditions in the Gulf of St. Lawrence, on the Scotian Shelf and in the Gulf of Maine using a regional climate model. Can Tech Rep Hydrogr Ocean Sci 334:xiii + 102 p

Lehmann MF, Barnett B, Gélinas Y, Gilbert D, Maranger RJ, Mucci A, Sundby B, Thibodeau B (2009) Aerobic respiration and hypoxia in the Lower St. Lawrence Estuary: Stable isotope ratios of dissolved oxygen constrain oxygen sink partitioning. Limnol Oceanogr 54:2157-2169

Lerman A, Lal D, Dacey MF (1974) Stokes' settling and chemical reactivity of suspended particles in natural waters. Suspended solids in water. Springer, Boston, p. 17-47

Levasseur M, Fortier L, Therriault J-C, Harrison P J (1992) Phytoplankton dynamics in a coastal jet frontal region. Mar Ecol Prog Ser 86:283-295

Levasseur ME, Therriault JC (1987) Phytoplankton biomass and nutrient dynamics in a tidally induced upwelling: the role of the NO_3: SiO4 ratio. Mar Ecol Prog Ser 39:87-97

Liu H, Chen M, Zhu F, Harrison PJ (2016) Effect of diatom silica content on copepod grazing, growth and reproduction. Front Mar Sci 3:89, doi:10.3389/fmars.2016.00089

Lomas MW, Glibert PM (2000). Comparisons of nitrate uptake, storage and reduction in marine diatoms and flagellates. J Phycol 36:903-913
Lund J, Kipling C, Cren E (1958) The inverted microscope method of estimating algal numbers and the statistical basis of estimations by counting. Hydrobiologia 11:143-170
Marie D, Partensky F, Jacquet S, Vaulot D (1997) Enumeration and cell cycle analysis of natural populations of marine picoplankton by flow cytometry using the nucleic acid stain SYBR Green I. Appl Environ Microb 63:186-193
Marie D, Simon N, Vaulot D (2005) Phytoplankton cell counting by flow cytometry. In: Andersen RA (ed) Algal culturing techniques. Academic Press London p. 253-267
McCarthy JJ (1972) The uptake of urea by natural populations of marine phytoplankton 1. Limnol Oceanogr 17:738-748
McCarthy JJ, Taylor WR, Taft JL (1977) Nitrogenous nutrition of the plankton in the Chesapeake Bay. 1. Nutrient availability and phytoplankton preferences: N nutrition of phytoplankton. Limnol Oceanogr 22:996−1011
McCrackin ML, Jones HP, Jones PC, Moreno-Mateos D (2017) Recovery of lakes and coastal marine ecosystems from eutrophication: A global meta-analysis. Limnol Oceanogr 62:207-518
Michaels AF, Silver MW (1988) Primary production, sinking fluxes and the microbial food web. Deep-Sea Res 35:473-490
Middelburg JJ, Nieuwenhuize J (2000) Nitrogen uptake by heterotrophic bacteria and phytoplankton in the nitrate-rich Thames estuary. Mar Ecol Prog Ser 203:13-21
Mucci A, Starr M, Gilbert D, Sundby B (2011) Acidification of Lower St. Lawrence Estuary bottom waters. Atmos Ocean 49:206-218
Neimi A (1979) Blue-green algal blooms and N:P ratios in the Baltic Sea. Acta Bot Fenn 110:57-61
Paasche E (1980) Silicon content of five marine plankton diatom species measured with a rapid filter method. Limnol Oceanogr 25:474-480
Paerl H, Valdes L, Joyner A, Piehler M, Lebo M (2004) Solving problems resulting from solutions: Evolution of a dual nutrient management strategy for the eutrophying Neuse River estuary, North Carolina. Environ Sci Technol 38:3068-3073
Paerl HW, Valdes LM, Peierls BL, Adolf JE, Harding LW (2006) Anthropogenic and climatic influences on the eutrophication of large estuarine ecosystems. LimnolOceanogr 51:448-462
Parsons TR, Maita Y, Lalli CM (1984) A manual of chemical and biological methods for seawater analysis. Pergamon Press, Oxford
Passow U, Alldredge AL (1995) A dye-binding assay for the spectrophotometric measurement of transparent exopolymer particles (TEP). Limnol Oceanogr 40:1326-1335
Passow U, Alldredge AL, Logan BE (1994) The role of particulate carbohydrate exudates in the flocculation of diatom blooms. Deep-Sea Res 41:335-357
Passow U, Shipe RF, Murray A, Pak DK, Brzezinski MA, Alldredge AL (2001) The origin of transparent exopolymer particles (TEP) and their role in the sedimentation of particulate matter. Cont Shelf Res 21:327-346

Pesant S, Legendre L, Gosselin M, Bauerfeind E, Budéus G (2002) Wind-triggered events of phytoplankton downward flux in the Northeast Water Polynya. J Mar Syst 31:261-278

Pinckney JL, Knotts ER, Kilber KJ, Smith EM (2020) Nutrient breakpoints for estuarine phytoplankton communities. Limnol Oceanogr 65:2999-3016

Pinckney JL, Paerl HW, Tester P, Richardson TL (2001) The role of nutrient loading and eutrophication in estuarine ecology. Environ Health Persp 109:699-706

Plourde J, Therriault J-C (2004) Climate variability and vertical advection of nitrates in the Gulf of St. Lawrence, Canada. Mar Ecol Prog Ser 279:33-43

Rabalais NN, Turner RE, Díaz RJ, Justić D (2009) Global change and eutrophication of coastal waters. ICES J Mar Sci 66:1528-1537

Raven JA, Waite AM (2004) The evolution of silicification in diatoms: inescapable sinking and sinking as escape? New Phytol162: 45-61

Redfield AC, Ketchum BH, Richards FA (1963) The influence of organisms on the composition of seawater. The sea 2:26-77. In: Hill MN (ed) The sea, Vol 2. Wiley, New York, NY,p 26-77

Rhee GY (1978) Effects of N:P atomic ratios and nitrate limitation on algal growth, cell composition, and nitrate uptake. Limnol Oceanogr 23:10-25

Riedel A, Michel C, Gosselin M (2006) Seasonal study of sea-ice exopolymeric substances on the Mackenzie shelf: implications for transport of sea-ice bacteria and algae. Aquat Microb Ecol 45:195-206

Romero N, Silverberg N, Roy S, Lovejoy C (2000) Sediment trap observations from the Gulf of St. Lawrence and the continental margin of eastern Canada. Deep-Sea Res Pt II 47:545-583

Roy S, Chanut J-P, Gosselin M, Sime-Ngando T (1996) Characterization of phytoplankton communities in the Lower St. Lawrence Estuary using HPLC-detected pigments and cell microscopy. Mar Ecol Prog Ser 142:55-73

Sañudo-Wilhelmy SA, Gobler CJ, Okbamichael M, GT Taylor (2006) Regulation of phytoplankton dynamics by vitamin B_{12}. Geophys Res Lett 33:L04604

Sarmiento JL, Gruber N (2006) Ocean biogeochemical dynamics. Princeton University Press, Princeton

Saucier FJ, Roy F, Gilbert D, Pellerin P, Ritchie H (2003) Modeling the formation and circulation processes of water masses and sea ice in the Gulf of St. Lawrence, Canada. J Geophys Res-Oceans 108(C8):3269, doi:10.1029/2000JC000686

Sherr EB, Sherr BF, Longnecker K (2006) Distribution of the bacterial and cell specific nucleic acid content in the Northeast Pacific. Deep-Sea Res 53:713-725

Simon M, Alldredge AL, Azam F (1990) Bacterial carbon dynamics on marine snow. Mar Ecol Prog Ser 65:205-211

Smith VH (1990) Nitrogen, phosphorus, and nitrogen fixation in lacustrine and estuarine ecosystems. Limnol Oceanogr 35:1852-1859

Smith VH, Schindler DW (2009) Eutrophication science: where do we go from here? Trends Ecol Evol 24:201-207.

Solorzano L, Sharp JH (1980) Determination of total dissolved phosphorus and particulate phosphorus in natural waters. Limnol Oceanogr 2:754-758

Thibodeau B, de Vernal A, Mucci A (2006) Recent eutrophication and consequent hypoxia in the bottom waters of the Lower St. Lawrence Estuary: Micropaleontological and geochemical evidence. Mar Geol 231:37-50

Tilman D (1982) Resource competition and community structure. Princeton University Press, Princeton

Tilman D, Kilham S, Kilham P (1982) Phytoplankton community ecology: the role of limiting nutrients. Annu Rev Ecol Syst 13:349-372

Tremblay J-É, Legendre L, Klein B, Therriault J-C (2000) Size-differential uptake of nitrogen and carbon in a marginal sea (Gulf of St. Lawrence, Canada): significance of diel periodicity and urea uptake. Deep-Sea Res Pt II 47:489-518

Van Meerssche E, Greenfield DI, Pinckney JL (2018) Coastal eutrophication and freshening: Impacts on *Pseudo-nitzschia* abundance and domoic acid allelopathy. Estuar Coast Shelf S 209:70-79

Villeneuve, V (2020) Caractérisation des variations saisonnière et spatiale des éléments nutritifs et de la prise de l'azote dissous dans l'estuaire du fleuve Saint-Laurent. Mémoire de maîtrise, Université Laval, Québec, Canada, 64 p.

Vincent WF, Bertrand N, Frenette JJ (1994) Photoadaptation to intermittent light across the St. Lawrence Estuary freshwater-saltwater transition zone. Mar Ecol Prog Ser 110:283-292

Wang R, Wang J, Xue Q, Sha X, Tan L, Guo X (2017) Allelopathic interactions between *Skeletonema costatum* and *Alexandrium minutum*. Chem Ecol 33: 485-498

Zhang S, Liu H, Ke Y, Li B (2017) Effect of the silica content of diatoms on protozoan grazing. Front Mar Sci 4:202, doi:10.3389/fmars.2017.00202

Ziadi N, Gagnon B, Cambouris A (2007) Utilisation des engrais minéraux azotés en grandes cultures : description des différentes formes et leurs impacts en agroenvironnement. Centre de Référence en Agriculture et Agroalimentaire du Québec, 1-29

Zubkov MV, Sleigh MA, Burkill PH (2001) Heterotrophic bacterial turnover along the 20 W meridian between 59°N and 37°N in July 1996. Deep-Sea Res Pt II 48:987-1001